CA/DOH/AIHL/SP-21

INVESTIGATION OF THE FILTRATION CHARACTERISTICS OF THE STACKED FILTER UNIT

Final Report

Interagency Agreement ARB A7-139-30

Prepared by

Walter John, Susanne Hering, Georg Reischl and Jerome J. Wesolowski

February 1980

Air and Industrial Hygiene Laboratory Section
Laboratory Services Branch
California Department of Health Services
2151 Berkeley Way
Berkeley, CA 94704

Submitted to:

Dr. Jack Suder
Research Section
State of California
Air Resources Board
P.O. Box 2815
Sacramento, CA 95812

The statements and conclusions in this report are those of the Contractor and not necessarily those of the State Air Resources Board. The mention of commercial products, their source or their use in connection with material reported herein is not to be construed as either an actual or implied endorsement of such products.

CONTENTS

FIGURES

TABLES

ABSTRACT

The characteristics of large pore Nuclepore filters have been investigated to evaluate the performance of the Stacked Filter Unit as a particle size - selective sampler. Pore densities, pore diameters, and filter thicknesses were measured for various lots of 5, 8 and 12 μm Nuclepore filters. A formula was developed for the pressure drop vs flow rate, this parameter being a good empirical indicator of filtration efficiency.

Nuclepore filtration efficiencies were measured by detecting the penetration of monodisperse particles with an optical counter. For liquid particles the efficiency increases slowly with flow rate, indicating that the principal filtration mechanism is interception. A theoretical calculation in the creeping flow approximation agrees well with the data. Efficiencies for solid particles are much lower than for liquid particles and decrease as the flow rate increases, showing the occurrence of particle bounce. Coating filters with grease greatly reduces the bounce effect. The efficiency and pressure drop change significantly for loadings of only a few particles per pore. Measurements of efficiency before and after loading with ambient particulate matter indicated optimum sampling results for grease-coated 8μm filters at a face velocity of 1.8 cm/s.

EXECUTIVE SUMMARY

This study is an evaluation of the Stacked Filter Unit, which is a size-selective particle sampler (Figure 1) consisting of a large pore-size (5-12μm) Nuclepore filter to collect large particles followed by a small pore-size (0.4μm) filter to collect the smaller particles which penetrate the first. The properties of the large pore size filters were investigated since these determine the particle size selection and were poorly known prior to this work.

Pore diameters, pore densities and filter thicknesses were measured for various lots of 5, 8 and 12 μm Nuclepore filters. Within a given lot, these parameters were uniform but there is sufficient variation between lots to require characterization of each lot for accurate filtration measurements. Since the pressure drop is an accurate empirical measure of the filter parameters, this was measured for various flow

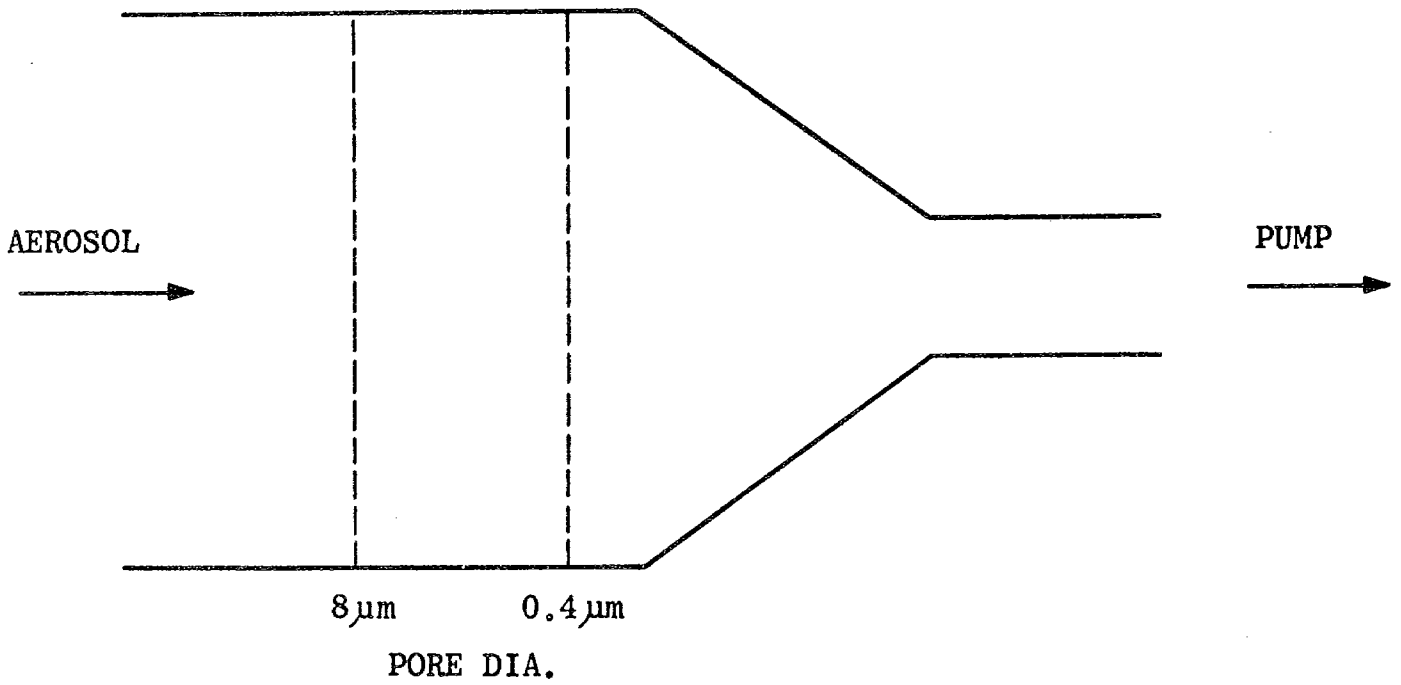

Figure 1. Diagram of stacked filter unit.

rates. A new theoretical formula was developed which predicts the pressure drop from the flow rate and filter parameters.

Filtration efficiencies were measured using accurately sized laboratory aerosol. For liquid particles, the efficiency increases weakly with flow rate, indicating that the principal filtration mechanism is interception. A theoretical calculation based on interception alone agrees well with the data. Efficiencies for solid particles are much lower than for liquid particles and decrease with increasing flow rate. This indicates that the solid particles tend to bounce from the filter surface and penetrate the pores. A thin grease coating on the filters was found to greatly reduce the bounce effect.

The filtration efficiency and pressure drop change significantly for loadings of only a few particles per pore. Measurements were made of the efficiency before and after loading with ambient particles. Optimum results were obtained with 8 μm grease-coated filters with a face velocity of 1.8 cm/s (1.5 L/min through a 47 mm filter).

It is concluded that the Stacked Filter Unit should not be regarded as a routine monitoring tool. Particles are sized geometrically rather than aerodynamically; the latter is preferred because it can be related to particle deposition in the lungs. The particle cutoff is more gradual than that of an impactor. Filters must be grease-coated to reduce particle bounce; the coating will complicate mass determination and chemistry. A low flow rate is necessary, implying a minimum sampling period of about one week. Within these limitations, the SFU is an inexpensive size-selective sampler which could be useful for special projects.

INTRODUCTION

The proper assessment of the adverse effects of particulate matter in ambient air requires particle size-selective sampling.[1] The particle size distribution is a determinant of the relative amount of toxic material deposited in various sites within the human respiratory system.[2] Visibility impairment also depends on particle size.[3] Particle size is an important parameter for the identification of sources of particles.[4] In addition to particle sizing, chemical analysis is essential for the evaluation of the toxicity and light scattering properties of the particulate matter.[4]

Instruments which can collect size-segregated samples for chemical analysis are available, for example, the dichotomous virtual impactor[5] and the cyclone.[6,7] However, a new sampler, the stacked filter unit (SFU),[8,9] has some attractive advantages, notably simplicity and low cost. The low cost allows deployment of a number of samplers for field studies over an extended area. The possible use of the SFU to generate data upon which control strategies will be based requires a thorough validation of the sampler's performance. Trial data obtained in the field so far has shown fair agreement between the SFU and other samplers.[8,9] While encouraging, such field tests are not sufficient assurance of satisfactory performance. Laboratory measurements at AIHL[10] revealed a serious problem in the use of the SFU. Solid particles were found to be sampled on the first filter with much less efficiency than liquid particles. The evidence indicates that solid particles have a fairly large probability of bouncing from the filter surface and then passing through the filter. Since the bounceoff effect increases with flow rate, it will be necessary to limit the flow rate to keep the sampling error within acceptable limits. In order to make a judicious choice of operating flow rate, it is desirable to have data taken at varying flow rates with both bouncy and sticky particles. It also desirable to have a determination of the effect of pore size on bounceoff.

Another important effect requiring investigation is the possible change of filtration efficiency with filter loading. Because the particles are deposited predominantly on the periphery of the pores, it is likely that the loading effect will be more important than with conventional filters.

The present study was designed to determine the filtration characteristics of the SFU using monodisperse laboratory aerosols under controlled conditions. The filtration efficiency for solid and liquid particles was determined as a function of particle size, air flow rate, filter pore size and particle loading. The measurements were extended to grease-coated filters, which might provide a solution to the particle bounce problem. The microscopic geometry of the Nuclepore filters was characterized, this information being essential to the interpretation of filtration measurements and to quality assurance. The filter support grid of the SFU was redesigned to reduce particle losses. These data provide a basis for interpretation of sampling data, for the establishment of the limitations of the SFU and for optimization of the operating parameters.

The Stacked Filter Unit

The possibility of using stacked filters for particle sizing was recognized by Spurny, et al.,[11,12] and investigated by Melo and Phillips.[13] Recently Parker, et al.,[9] and Cahill, et al.,[8] suggested the use of two stacked filters for ambient air sampling with an approximately "respirable"[14] cutoff, i.e., a gradual cutoff with a 50% cutpoint near 3.5 µm. The SFU consists of two Nuclepore filters in a stack so that the air passes first through a large pore size filter where large particles are deposited. Subsequently the finer particles penetrating the first filter are removed on the second, small pore size filter. Parker, et al.[9] employed a 12 µm pore size for the first filter while Cahill, et al.[8] used an 8 µm pore size.

Nuclepore* filters are manufactured by a special process. The pores are initiated by radiation damage caused by fission fragments bombarding the polycarbonate plastic. Sodium hydroxide is then used to etch the holes to the final size. The resulting filter consists of cylindrical holes passing straight through the plastic. This geometry gives rise to the unique properties of the filter including the possibility of sizing the particles by selective penetration. Nuclepore filters are highly suitable for automated x-ray fluorescence analysis which yields the concentrations of approximately 20 elements including sulfur, lead and a number of metals.[15] The particles are deposited on an exposed surface rather than inside the random structure of conventional membrane filters, simplifying the x-ray absorption correction. The Nuclepore polycarbonate material has very low blank values, is non-hygroscopic and quite strong.

It was realized early that the Nuclepore geometry is amenable to theoretical calculation of the filtration efficiency.[11] In fact, considerable success was achieved for particles small compared to the pore size. For particles comparable to the pore size the theory was deficient due to inadequate treatment of interception or the sieving action of the filter. However, this is probably the most important filtration mechanism for the SFU, as indicated by preliminary experimental and theoretical work on the SFU conducted at AIHL.[10]

---

* Nuclepore Corp., Pleasanton, CA.

PHYSICAL CHARACTERIZATION OF NUCLEPORE FILTERS

Detailed measurements were made on the physical parameters of the Nuclepore filters for use in the interpretation of filtration efficiencies. Data were obtained on variations from filter to filter within a batch and also between batches for quality assurance purposes. Parameters measured include pore size, pore density, areal distribution of holes, thickness and pressure drop vs. flow rate.

Nuclepore Numbering System

It is helpful to understand the filter batch number system, which was supplied by courtesy of the Nuclepore Corp. For example, lot number 51C7B4 denotes:

5 1	$1 \cdot 10^5$ pores/cm^2
C	roll number for reactor exposure
7	year 1977
B	subroll for etching
4	wrap number

The first two digits give the pore density measured at the factory. Rolls are numbered for reactor exposure which determines the pore density. Etching is carried out in subrolls; this determines the pore size. The wrap number designates a portion of the subroll.

Pore Size

The pores were examined in a Reichert Zetoplan microscope with a 63 X objective and a 12.5 X eyepiece. The eyepiece reticle scale was calibrated against a stage micrometer. The smallest scale division corresponded to 1.5 µm on the pore. For each filter batch 10 pores selected at random were sized on each of 10 filters. The average pore sizes and standard deviations are listed in Table 1. The standard deviations are larger than the estimated measurement accuracy of ± 0.2 µm. The pore size distributions were skewed towards smaller diameters. Average pore sizes were consistently smaller than the nominal pore size, a consequence of the manufacturer's desire to limit penetration to particles smaller than the nominal pore size.

One 8 µm pore size filter from batch number 51C7B4 was sized on both sides for

comparison. The results were 7.47 ± 0.53 μm on the shiny side and 7.29 ± 0.56 μm on the dull side. Therefore no significant difference was found. This does not eliminate the possibility that the pore diameter is different within the filter.

TABLE 1. Nuclepore filter parameters

Nominal Pore Size μm	Lot Number	Pore Density $10^5 cm^{-2}$	Pore Diameter μm	Porosity %	Doublets %
12	51C7C20	0.96 ± 0.25	11.1 ± 0.6	9.3	13.2
"	51C7C21	0.90 ± 0.21	11.0 ± 0.6	8.5	12.6
"	51C7C22	0.94 ± 0.22	11.0 ± 0.7	8.9	12.4
"	51C7C23	0.94 ± 0.27	10.8 ± 0.6	8.6	13.4
"	51G6C10	1.13 ± 0.28	10.6 ± 0.5	10.1	14.5
"	51C7C6-1*	0.95 ± 0.26	9.9 ± 0.4	7.3	9.9
"	51C7C6-2	0.96 ± 0.25	9.6 ± 0.2	7.0	10.7
"	51G6C2-1	1.22 ± 0.29	10.9 ± 0.3	11.4	15.7
"	51G6C2-2	1.26 ± 0.26	11.0 ± 0.2	12.0	15.5
8	51C7B4	0.93 ± 0.26	7.5 ± 0.6	4.1	6.2
"	51A7B6	1.11 ± 0.34	7.3 ± 0.8	4.7	8.4
"	51A7B12	1.07 ± 0.26	7.9 ± 0.3	5.2	7.5
"	51D7B83	0.82 ± 0.23	7.4 ± 0.5	3.5	6.6
"	51D7B75	0.88 ± 0.23	6.9 ± 0.4	3.3	5.5
"	51D7B55	0.84 ± 0.26	6.4 ± 0.5	2.7	4.3
"	51E6A5	1.00 ± 0.26	6.2 ± 0.2	3.0	6.6
5	54E7A126	2.69 ± 0.8	4.4 ± 0.3	4.0	7.1
"	54E7A129	2.84 ± 1.0	4.0 ± 0.3	3.5	5.9
"	54A8A35	3.74 ± 0.9	5.2 ± 0.2	7.8	11.7
"	54A8A43	4.01 ± 1.1	4.9 ± 0.2	7.5	12.5
"	54A8A57	4.21 ± 1.1	4.7 ± 0.2	7.4	11.9

*The dashed numbers are used to designate boxes with the same lot number.

Pore Density

Pore densities were evaluated by counting pores in a field defined by a partially closed field iris diaphram. On each of 10 filters in a batch, fields were located in 10 radial zones of equal area with the azimuthal angle selected by random numbers. The total number of pores counted in each batch was of the order of 1000. Results are listed in Table 1.

From the measured pore density and pore size the porosity was calculated for each batch and listed in Table 1. The porosity varies by almost a factor of 2 for a given filter type (nominal diameter 5, 8 or 12 μm).

Areal Distribution of Pores

Initiation of the pores by fission fragments should produce pores randomly located on the filters. The observation of cases of many overlapping pores raised a question about the randomness of the areal distribution. The manufacturer reported some defective batches in earlier years. Therefore a check on the areal pore distribution was made.

The microscopic filter image was displayed on a TV monitor with a circle on its face to define a field which typically contained about 10 holes. The fields were chosen as described above for the pore density measurements. Ten fields were counted on each of 10 filters for a total of about 1000 pores in a batch. Overlapping holes were recorded as doubles, triples, etc.

From the data, N_n, the number of fields with n pores can be tabulated. If the distribution were random, the expected number of fields with n pores, E_n, will be given by the Poisson distribution:

$$E_n = \frac{N_T(\bar{n})^n e^{-\bar{n}}}{n!}$$

where N_T is the total number of fields and $\bar{n}$ is the average number of pores per field. To evaluate the goodness of fit, the chi-squared test was applied by calculating

$$\chi^2 = \sum_n \frac{(N_n - E_n)^2}{E_n}$$

For example, for batch 51C7B4, $\chi^2 = 11.0$ with 13 degrees of freedom. From statistical tables, it is found that the probability of this value to occur randomly is 50 to 70%. Normally the probability would have to be less than 1% before the departure from randomness would be considered significant. All batches listed in Table 1 passed this test.

Another test of randomness which also yields information of some practical interest

is afforded by the data on pores consisting of overlapping holes. For the purposes of this discussion a hole signifies a single, cylindrical hole. We define a pore to be the opening in a filter which may consist of a single hole or more than one overlapping holes. A doublet is then counted as one pore with hole multiplicity n = 2. The overlap area for a doublet is well defined. If the centers of two holes are separated by a distance less than their diameter, D, they overlap, otherwise, they do not. The area of the overlap region for a doublet is

$$A_2 = \pi D^2$$

The average number of holes in A_2 is given by:

$$n_2 = n_A \cdot \pi D^2$$

where n_A is the average number of holes per unit area. For a random distribution, the probability that 2 holes will be within A_2, i.e., that they will overlap is

$$f(n) = \frac{(n_2)^n e^{-n_2}}{n!}$$

with n = 2. The triplet overlap probability can also be calculated from the above equation with n = 3 although this will only be approximate since the overlap area for a triplet, A_3, is larger than A_2. The percentage, P, of pores with overlap multiplicity n is given by

$$P = 100\ f(n) / \sum_{n=1}^{\infty} f(n)$$

Note that the sum excludes n = o.

In Table 2, the percentage of pores with overlapping holes calculated from the above theory is compared to measurements on three filter batches. The agreement is quite good. The observed percentage of doublets for each filter batch is listed in Table 1.

TABLE 2. Percentage of pores with overlapping holes

Filter Lot No.	Average Pore Dia, μm	Overlap Multiplicity n	Number Observed	% Observed	% Theory
51C7C20	11.1	1	956	84.9	83.3
		2	149	13.2	14.9
		3	21	1.9	1.8
51C7B4	7.5	1	1,165	93.4	91.9
		2	77	6.2	7.7
		3	5	0.4	0.4
54A8A43	4.9	1	1,136	86.4	85.4
		2	165	12.5	13.3
		3	14	1.1	1.3

Filter Thickness

The thickness of the filters was measured in two different ways, by weighing and by microscope. The first method consisted of weighing 10 filters from each batch on a Mettler balance. The thickness was caculated, knowing the diameter (47 mm), the density of the plastic, 1.20 g/cm^3, and the porosity. The second method consisted of successively focusing on the top and bottom of the filter and reading the vertical displacement on the microscope knob. It was found helpful to apply 0.5 μm latex spheres to the filter since the bottom surface was indistinct. The observed displacement was then multiplied by the index of refraction, 1.585, to obtain the thickness of the plastic.

From the plot in Figure 2, it can be seen that the two methods yielded data in good agreement. The slope of the line, -1.00, indicates that the thickness decreases at the same rate as the diameter increases, as expected from the etching process.

Theory of Pressure Drop

The usual calculation of the pressure drop across a filter considers only the pressure drop within the filter. This has been found to be inadequate for Nuclepore filters of large pore size; for example, the pressure drop calculated for 12 μm pores is less than

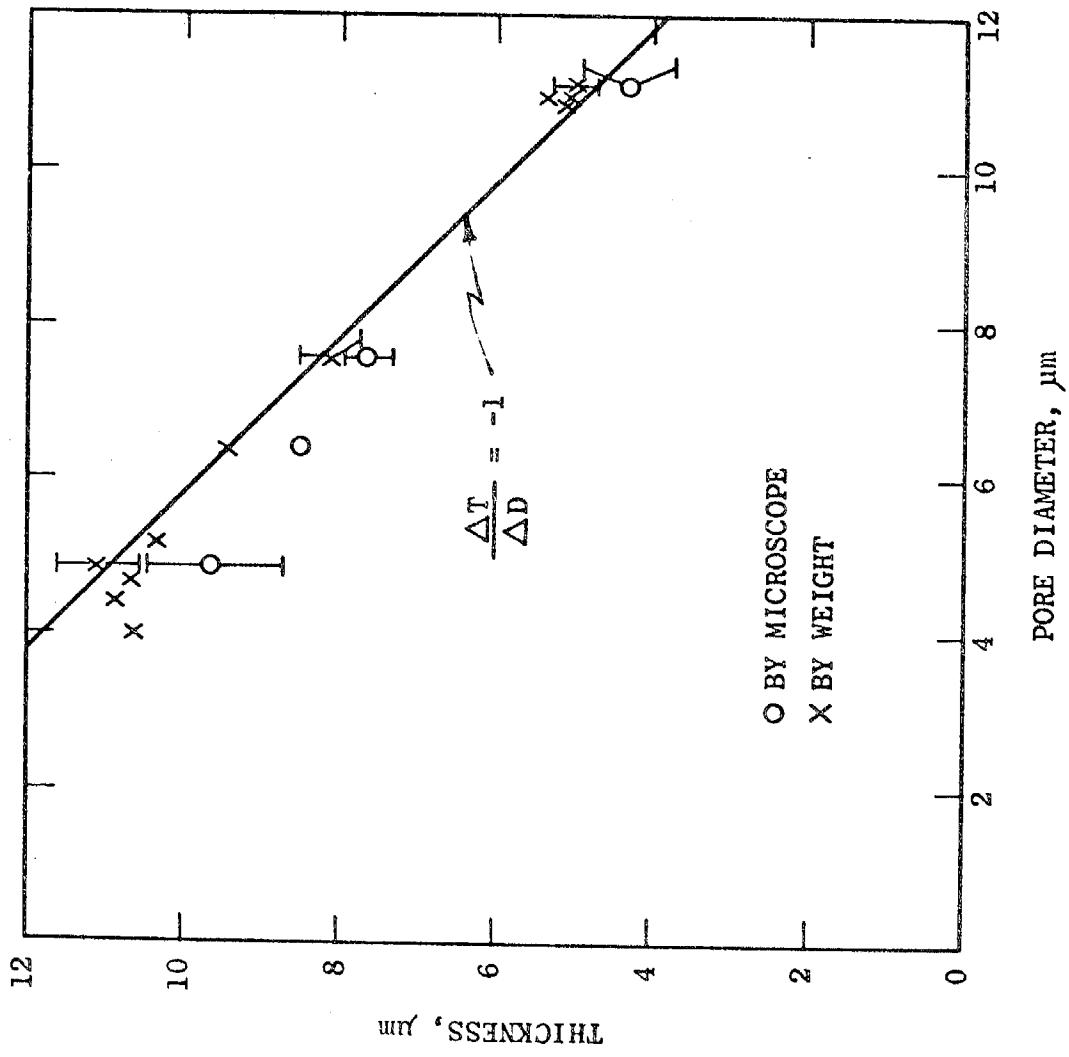

Figure 2. Thickness of Nuclepore filters vs. pore diameter. The line was fitted to the data by eye.

half of that observed. The theory presented here incorporates another term to include the pressure drop from viscous flow of the air as it converges to the pore on one side of the filter and diverges on the other side. This external pressure drop, ΔP_E, can be derived in the creeping flow approximation[16] for flow through an isolated orifice in an infinitely thin plate:

$$\Delta P_E = \frac{24Q\eta}{D^3}$$

where Q is the flow rate per pore, η the fluid viscosity and D the pore diameter.

The face velocity v may be introduced by:

$$Q = \frac{F}{NA} = \frac{v}{N}$$

where F is the total flow rate, N the number of pores/cm^2 and A the exposed area. Therefore,

$$\Delta P_E = \frac{24v\eta}{ND^3} \qquad (1)$$

The internal pressure drop, ΔP_I, across a cylindrical Nuclepore pore of length L (filter thickness) is given by the Hagen - Poiseuille formula,[17] with a slip correction.

$$\Delta P_I = \frac{128Q\eta L}{\pi D^4 (1 + 11.0\ \ell/D)} \qquad (2)$$

$$= \left(\frac{16}{3}\frac{L}{\pi D}\right) \Delta P_E \left(\frac{1}{1 + 11.0\ \ell/D}\right) \qquad (3)$$

Where ℓ is the mean free path of the air molecules. Thus ΔP_I is comparable to ΔP_E when the pore length is comparable to D, a condition realized for the large pore sizes.

The total pressure drop, ΔP_T, is obtained by adding the external and internal pressure drops. This neglects second order effects at the pore entrance.

$$\Delta P_T = \Delta P_E + \Delta P_I \qquad (4)$$

Equation (4) shows that the pressure drop is not simply related to the porosity, but must be calculated from several filter parameters.

Pressure Drop Measurements

Pressure drops were measured with the apparatus described below in connection with efficiency measurements. The filters were unbacked and the pressure was observed with a manometer. The pressure drop was measured vs. flow rate. The typical set of data in Figure 3 shows that the pressure drop varies linearly with face velocity as predicted by Equation 4.

Pressure drop data for a number of filter lots are listed in Table 3. These data were taken in the course of the efficiency measurements. The experimental pressure drops are the average for a number of filters from the given lot and the standard deviation is quoted.

The comparison of experiment to theory displayed in Table 3 shows that Equation 4 predicts the pressure drop within 3% and 10% accuracy for 8 and 12 μm pore diameters respectively. There is a trend towards overestimation of the pressure drop for smaller pores. The good agreement between the calculated and observed pressure drops is an overall check of the accuracy of the measured filter parameters and air flow rates.

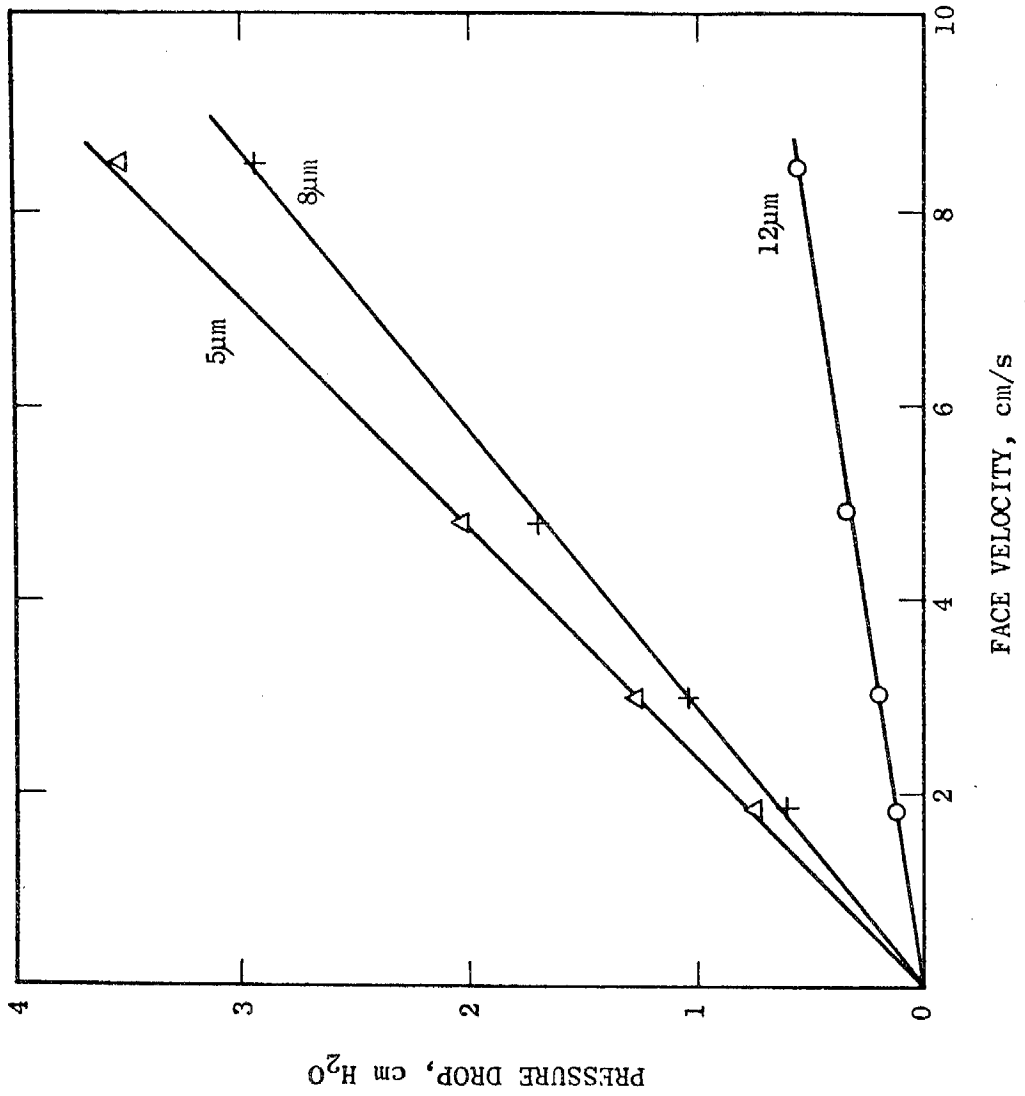

Figure 3. Pressure drop across 5, 8 and 12 µm pore diameter filters vs. face velocity.

TABLE 3. Pressure drops observed and calculated for Nuclepore filters for a face velocity of 8.4 cm/s.

Nominal Pore Size µm	Lot Number	Pressure Drop, cm H_2O Theory	Exp.	Theory/Exp.	Average $\frac{\text{Theory}}{\text{Exp.}}$
12	51C7C20	0.49	0.55 ± 0.02	0.89	
"	51C7C21	0.56	0.56 ± 0.02	1.00	0.98
"	51C7C22	0.52	0.52 ± 0.02	1.00	±0.06
"	51C7C23	0.55	0.53 ± 0.02	1.04	
8	51C7B4	2.48	2.74 ± 0.13	0.91	0.99
"	51D7B55	5.53	5.21 ± 0.13	1.06	±0.11
5	54A8A43	3.38	3.30 ± 0.10	1.02	
"	54E7A129	9.73	8.8 ± 0.7	1.11	
"	54E7A126	7.37	8.5 ± 0.3	0.87	1.07
"	54A8A35	2.82	2.49 ± 0.13	1.13	±0.14
"	54A8A57	3.53	2.84 ± 0.18	1.24	

FILTRATION EFFICIENCIES

Experimental Methods

The experimental arrangement used to measure filtration efficiencies is diagramed in Figure 4. Monodisperse (σ_g <1.02) particles were produced by a vibrating orifice aerosol generator[18]. Particle charges were reduced to Boltzmann equilibrium levels by a Kr-85 beta ray source. This was followed by an ion sweeper with a weak electric field (30 V/cm) to eliminate possible charging effects from residual ions. The aerosol was then sampled from the plenum by Climet optical counter #1 to monitor the particle concentration. Aerosol was pumped through the Nuclepore filter by Climet optical counter #2 which measured the particle penetration through the filter.

Four different flow rates through the Nuclepore filters were achieved by the apparatus shown in Figure 5. With no dilution air, the maximum flow rate was determined by the normal Climet flow rate of 7.2 L/min. When 3.1 L/min of dilution air was introduced, the flow through the filter was 4.1 L/min. To obtain even lower flow rates, the Climet flow rate was reduced to 4.0 L/min. At the lower flow rate the

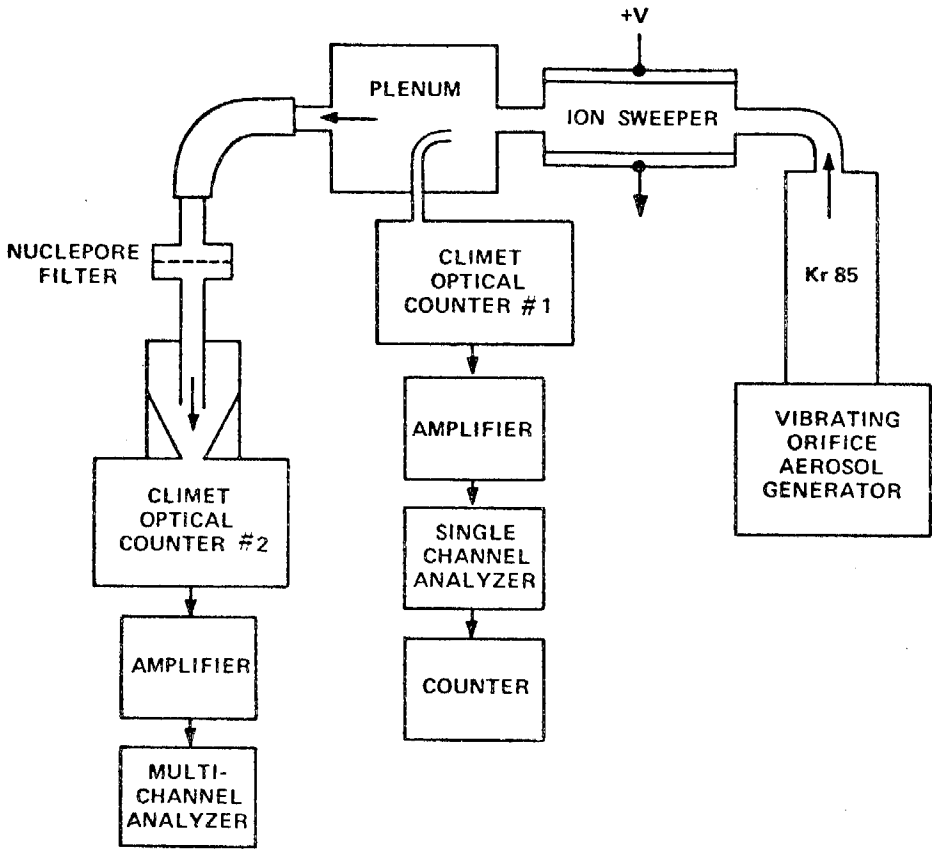

Figure 4. Experimental arrangement for filtration efficiency measurements.

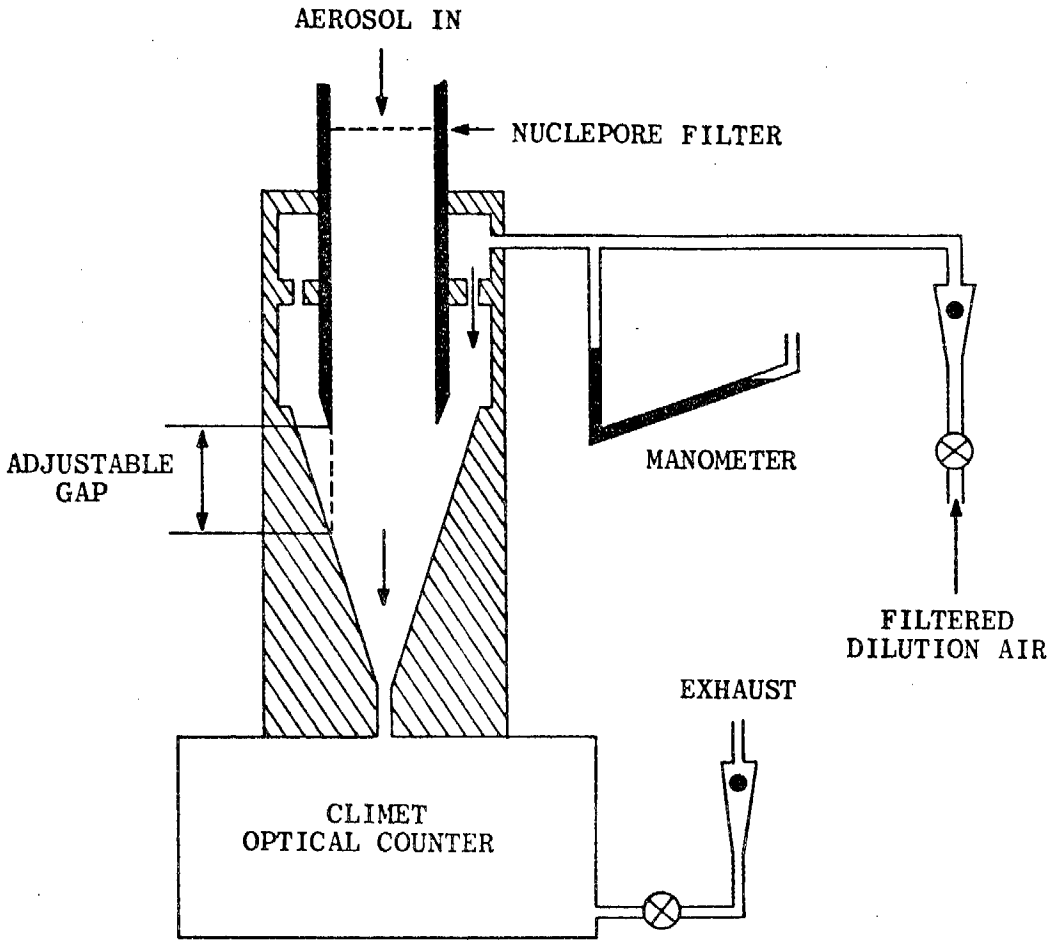

Figure 5. Dilution air system for filtration efficiency measurements.

pulses are larger for a given particle diameter, necessitating a recalibration of the Climet with latex aerosol. When dilution air was used, the adjustable tube (Figure 5) was positioned vertically through the O-ring seals so that the velocities of the merging air streams were matched. The dilution air formed a clean air sheath around the aerosol stream. The air flow rates were set by the rotameters shown in Figure 5 to calibrate the air flow; a wet test meter was placed at the Nuclepore filter position to measure the incoming flow. A further consistency check on relative flow rates was afforded by the pressure drop across the filter which is linear with flow rate.

The 47mm Nuclepore filters were clamped in stainless steel holders. As shown in Figure 6, the filters were unbacked. One O-ring sealed to the filter surface while a second O-ring sealed to the flange, eliminating any possibility of leakage. The filter holder was then clamped between two O-rings in the aerosol exposure apparatus; the inside diameters of the pipes matched the filter opening to provide a smooth channel for the aerosol flow. The filter holders could be changed in a matter of seconds by means of the hinged arrangement. Loading of filters into the holders was facilitated by the fixture shown in Figure 7 which provided a gentle holdown vacuum.

Liquid particles having diameters $\geq$1.6 µm were generated by atomization of aqueous solutions of glycerol. Glycerol droplets smaller than 1.6 µm were observed (via the optical counters) to have a size dependent on the holdup time, presumably due to evaporation. Therefore, for diameters less than 1.6 µm, dioctyl pthalate (DOP) in isopropyl alcohol solution was atomized. Particle size was based on calculation from the operating parameters of the vibrating orifice and the solution concentration. Relative sizes were further determined from the optical counter pulse height vs. diameter curve. Solid particles were generated from aqueous solutions of potassium biphthalate (KHP). Potassium biphthalate forms a white, bouncy particle. Because the particle dries with appreciable void space, the diameters were determined directly by sizing in an optical microscope. Again, relative sizes were checked with the optical counters. The particle mass can be calculated from the aerosol generation parameters. This mass, in combination with the microscopic size, yields the effective density of the potassium biphthalate particles which turns out to be almost exactly 1.0 (0.98 $\pm$ 0.03). Therefore the aerodynamic diameter is equal to the microscopic diameter.

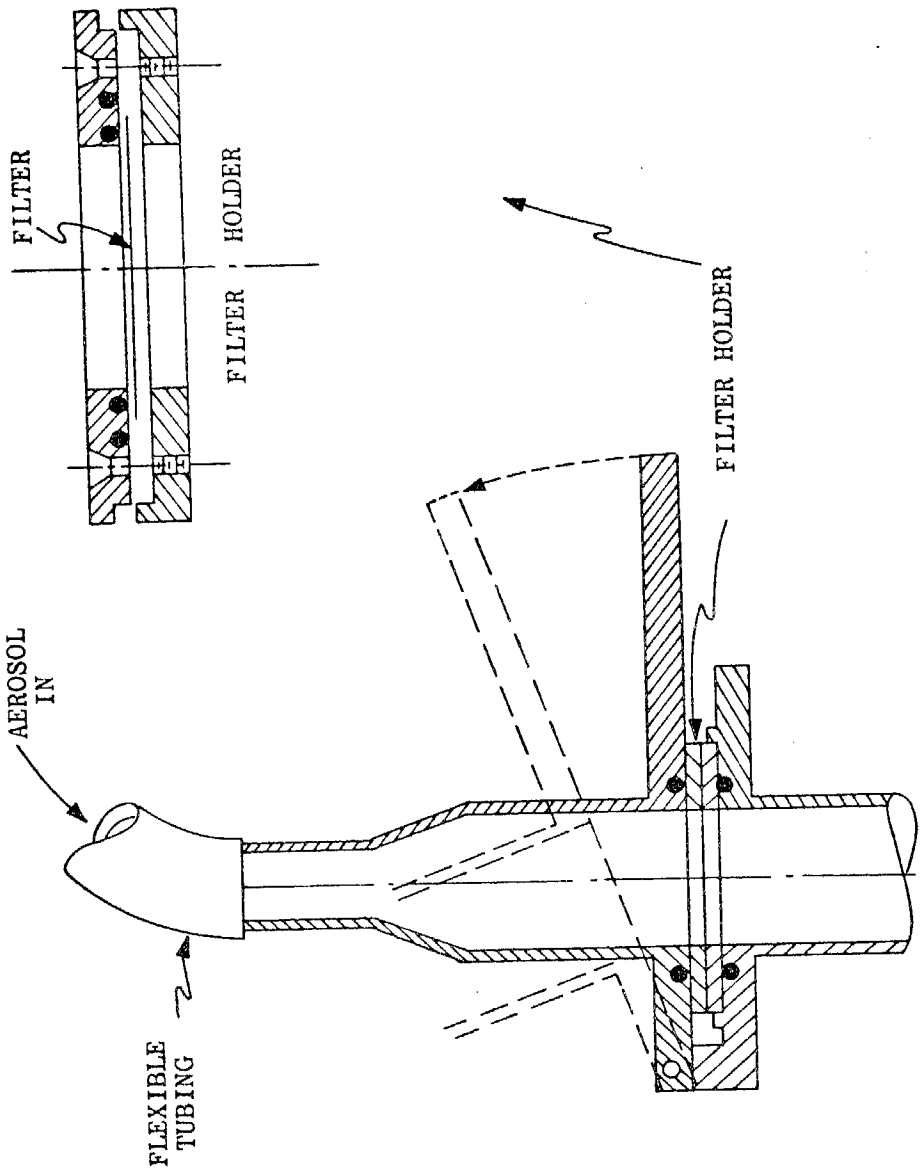

Figure 6. Details of the filter holder.

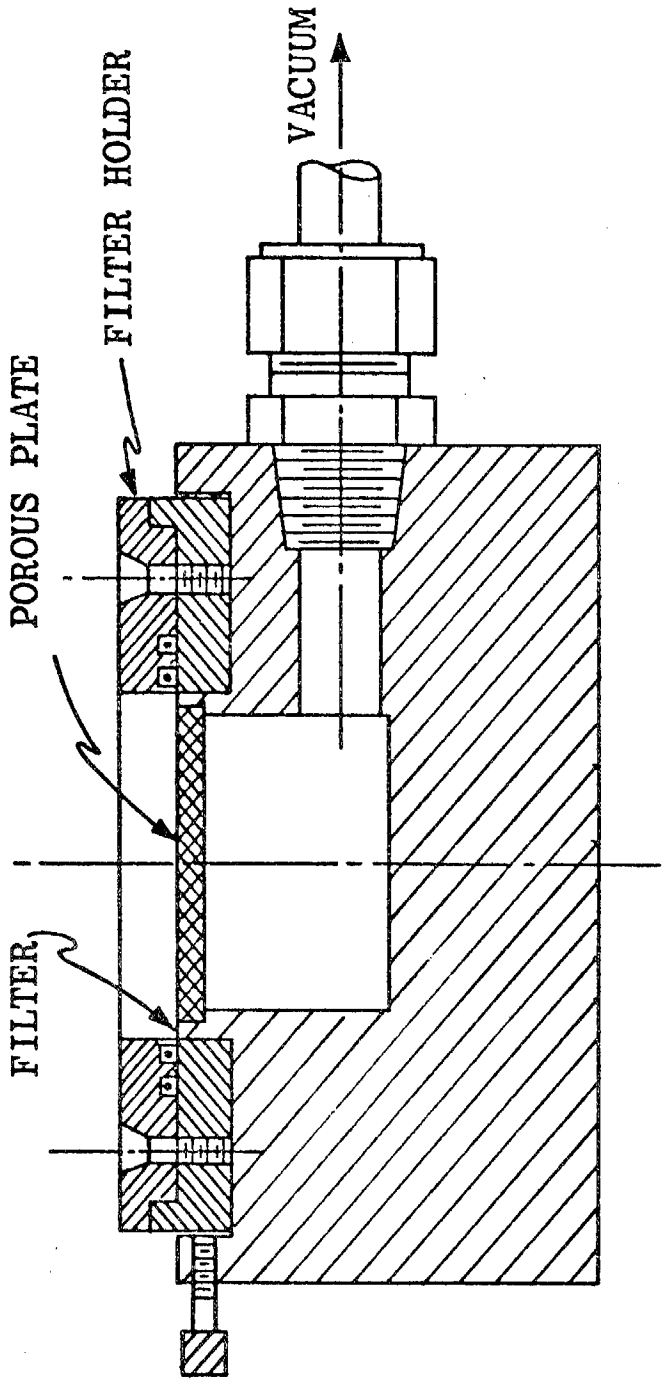

Figure 7. Fixture for loading Nuclepore filters into the filter holder.

Measurements were also made with polystyrene latex particles (PSL) having diameters of 1.305, 0.801 and 0.500 µm generated with a DeVilbiss nebulizer.

The filtration efficiency, e, was determined from:

$$e = 1 - \frac{N_2}{N_1}$$

Where N_1 is the number of particles /L incident on the filter and N_2 is the number/L penetrating the filter. An efficiency measurement consisted of taking a one-minute count on Climet #2 with an empty filter holder in place. N_2 was then determined by a second one-minute count with a filter in place. A third count was taken with an empty filter holder. The average of the first and third counts gave N_1. It was found that the precision of the results was improved slightly by normalizing the counts on Climet #2 to the counts on Climet #1 taken simultaneously.

Variation of Efficiency with Filter Parameters

The first series of tests were designed to investigate the variation of filtration efficiency due to variation of filter parameters from filter to filter within a filter lot and from lot to lot. For each nominal pore size the particle size and flow rate were held constant for a series of efficiency and pressure drop measurements. The particle sizes were chosen to give efficiencies in the 50 to 70% range; again, these filters are to be used for the first size-selective filtration stage.

The data listed in Table 4 illustrates both aspects of the variations. The first aspect, variation from filter to filter within a lot, is evident from the standard deviations in efficiency and pressure drop. The standard deviation in efficiency is generally less than 1% which attests to the small variation between filters as well as to the precision of the measurements. The standard deviation in pressure drop is also uniformly small. Thus, within a given filter lot, the reproducibility of filtration efficiency is entirely satisfactory.

By contrast, the variation in filtration efficiency from lot to lot is much larger. For example, for a nominal 8 µm pore size, the efficiency for 2.6 µm particles ranged from 55 to 66%. The pressure drop likewise showed a large variation; in fact, the filtration efficiency increases monotonically as the pressure drop increases. Therefore the

pressure drop is a good empirical indicator of efficiency although the relation between efficiency and pressure drop is analytically complex. The data show that accurate work requires knowledge of the lot number and the corresponding filter parameters.

TABLE 4. Filtration efficiency and pressure drop for glycerol particles of a given size and a face velocity of 8.4 cm/s.

Nominal Pore Dia. µm	Lot Number	Particle Dia. µm	No. of Filters Tested	Average Efficiency ± Std. Dev.,%	Average Pressure Drop cm H_2O
12	51G6C2	4.4	2	67	0.36
"	51G6C10	"	1	69	0.46
"	51C7C20	"	6	69.8 ± 0.8	0.51 ± 0.01
"	51C7C22	"	8	69.9 ± 0.7	0.52 ± 0.02
"	51C7C23	"	10	70.7 ± 0.6	0.53 ± 0.02
"	51C7C21	"	8	71.4 ± 0.9	0.56 ± 0.02
"	51C7C6	"	2	77	0.81
8	51A7B12	2.6	1	55	2.2
"	51A7B6	"	1	56	2.7
"	51C7B4	"	15	56.0 ± 0.8	2.7 ± 0.1
"	51D7B83	"	1	58	3.4
"	51E6A5	"	1	65	3.7
"	51D7B55	"	1	66	5.1
5	54A8A35	1.7	5	56.8 ± 0.6	2.5 ± 0.1
"	54A8A57	"	4	62.1 ± 0.6	2.9 ± 0.2
"	54A8A43	"	4	63.6 ± 0.3	3.3 ± 0.1
"	54B4A206	"	4	67.8 ± 0.3	3.6 ± 0.1
"	54E7A126	"	4	75.5 ± 0.5	8.5 ± 0.3
"	54E7A129	"	4	76.5 ± 1.2	8.8 ± 0.7

Filtration Efficiencies For Liquid and Solid Particles vs. Particle Size and Face Velocity

Extensive measurements were made on filters from one lot of 20 µm, one lot of 5 µm and two lots of 8 µm filters, the latter two chosen to span the differing filter parameters. Filters were changed after each measurement at a given particle size to avoid any loading effects and to ensure a representative sampling of the filters. Face velocities were 1.8, 2.9, 4.8, and 8.4 cm/s (1.5, 2.5, 4.1 and 7.2 L/min through 47 mm filters). The results for both solid and liquid particles are presented in Figure 8 - 11.

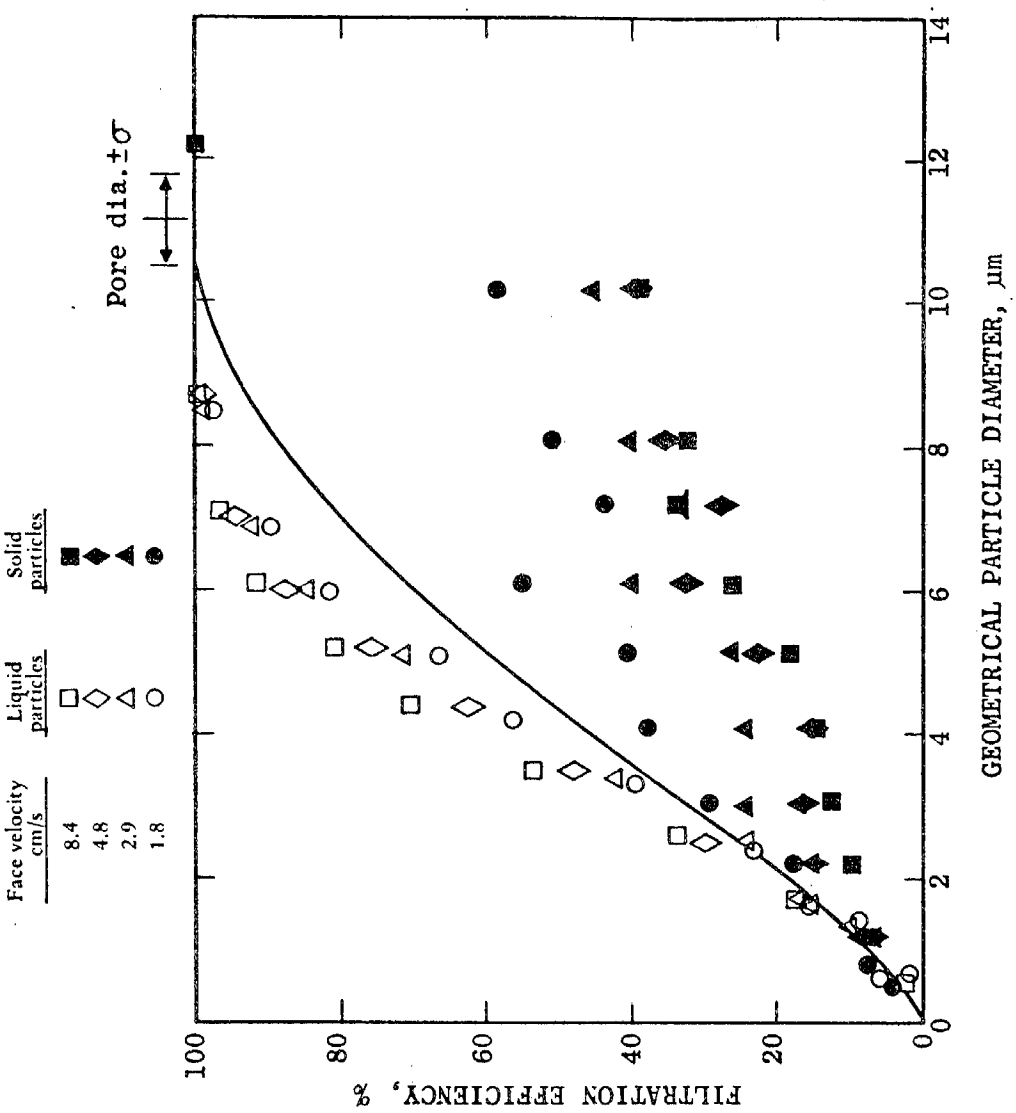

Figure 8. Filtration efficiency vs. particle diameter for liquid and solid particles at several flow rates through 12 µm Nuclepore filters from lot 51C7C20. The line is a theoretical calculation of particle filtration by interception only.

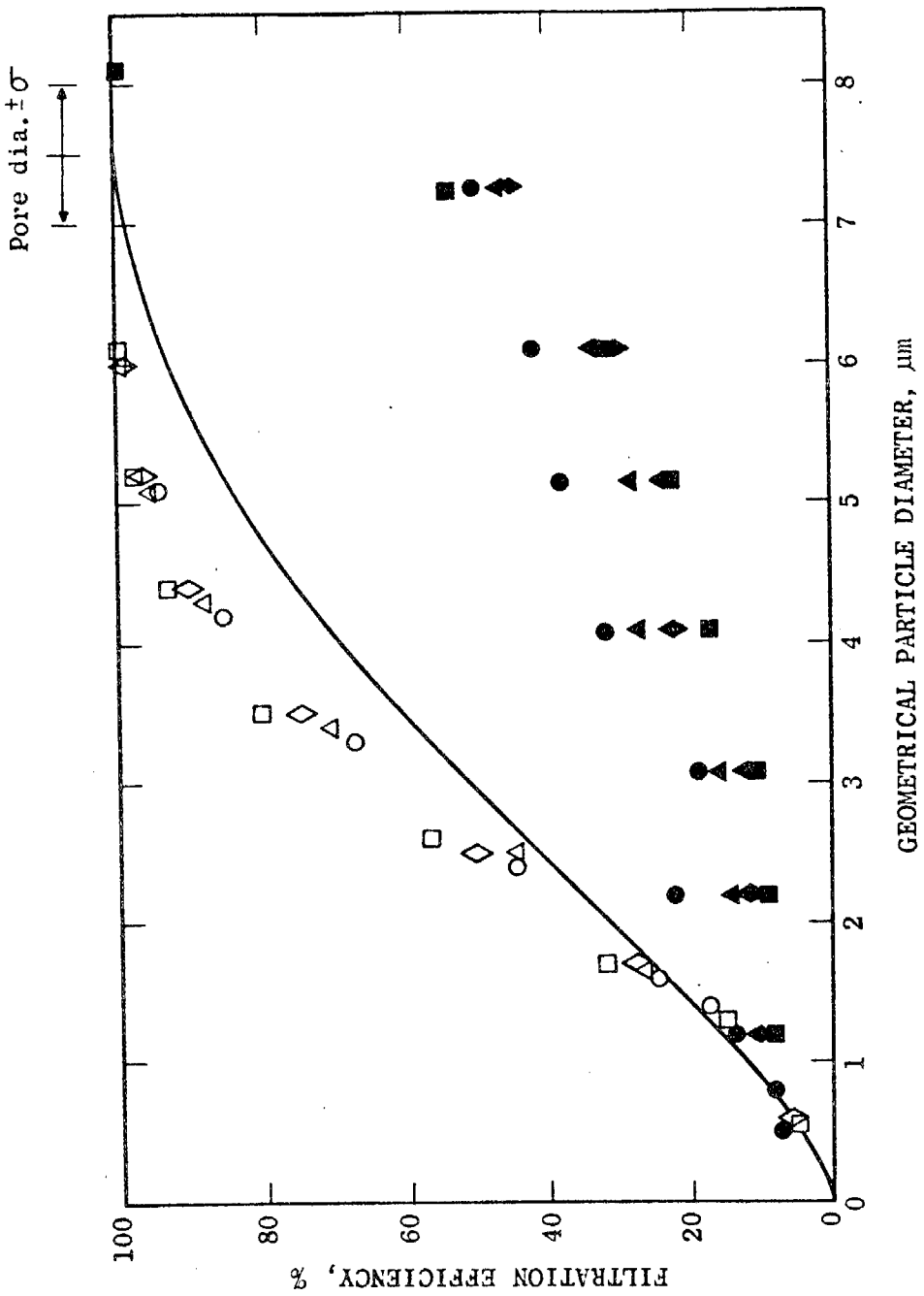

Figure 9. Filtration efficiencies for 8 µm Nuclepore filters from lot 51C7B4. Data symbols and line are explained in Figure 8.

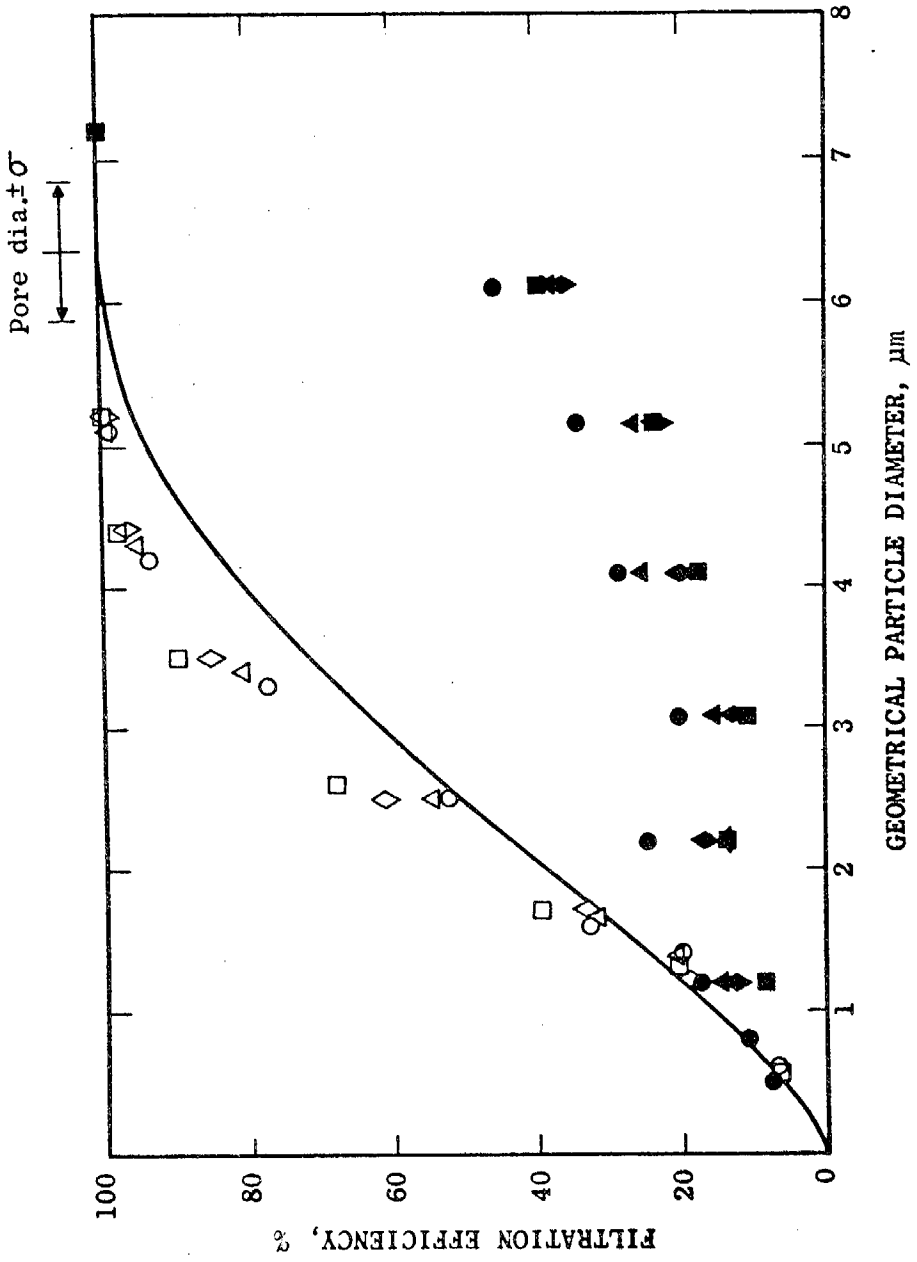

Figure 10. Filtration efficiencies for 8 μm Nuclepore filters from lot 51D7B55. Data symbols and line are explained in Figure 8.

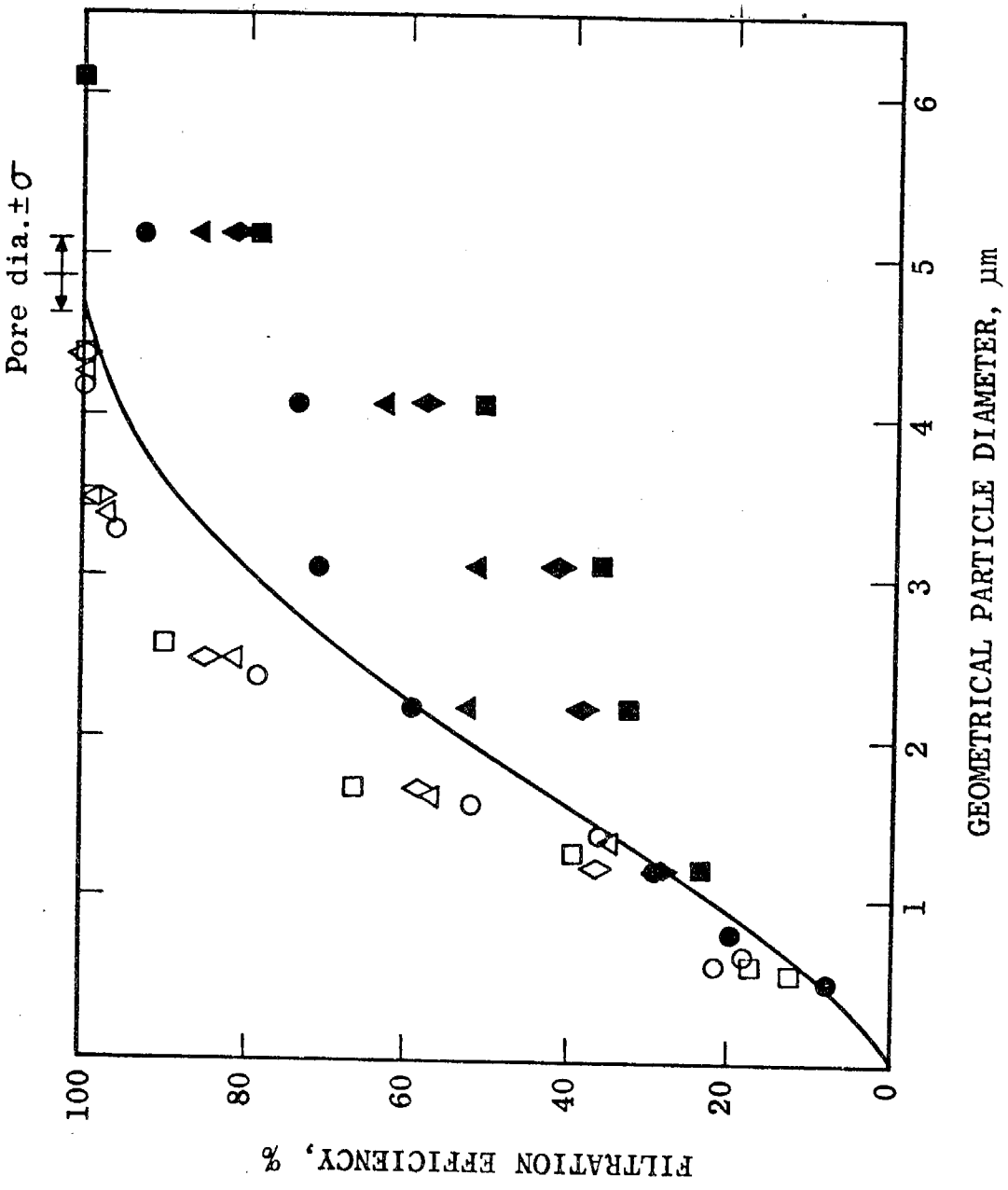

Figure 11. Filtration efficiencies for 5 μm Nuclepore filters from lot 54A8A43. Data symbols and line are explained in Figure 8.

Discussion

The efficiencies for liquid and solid particles were found to be nearly the same for small particles but differed markedly for larger particle diameters until the pore size was approached. For liquid particles, filtration efficiency increased slowly with increasing face velocity as expected from inertial impaction. However, for solid particles the efficiency decreased with increasing face velocity. The solid particle results are consistent with the occurrence of particle bounce. Examination of the filters under a microscope revealed that the particle deposits were concentrated on the peripheries of the pores as expected from the convergence of the airflow streamlines to the pores. Therefore, if a particle bounces, it has a high probability of passing through the pore.

The curves in Fig. 8 - 11 are from a theoretical calculation of the filtration efficiency including interception only. The fair agreement between the data points for liquid particles and the calculated interception efficiency as well as the rather small increase of efficiency with face velocity shows that interception is the principal filtration mechanism. The geometrical particle diameter is therefore the appropriate variable rather than the aerodynamic diameter. By dividing the geometrical particle diameter by the pore diameter a dimensionless parameter is obtained, allowing the data for all pore sizes to be included in the same plot. This has been done in Fig. 12 for the lowest face velocity, 1.8 cm/s. It can be seen that the data for all pore sizes show the same dependence on the dimensionless particle size. For small particle size the data agree well with the theoretical interception curve. The measured efficiency is systematically slightly larger than the theoretical efficiency at larger particle sizes, which may be due to changes in the air flow pattern in the presence of the particle, an effect not taken into account by the theory.

When used as the coarse filter in the SFU, the 12 μm pore filters give a reasonably good approximation to the industrial hygiene "respirable" cutoff curve[14] with a 50% cutpoint at 3.8 μm (1.8 cm/s face velocity). The 8 μm pore filters have a cutoff curve shifted to smaller sizes, the 50% cutpoint being at 2.6 μm (1.8 cm/s). This is practically the same as the 2.5 μm cutpoint currently recommended[19] by the Environmental Protection Agency for ambient sampling. However, the cutoff of particles >2.5 μm is not as sharp as that of the dichotomous virtual impactor. The 5 μm pore size filters give a 50% cutpoint even lower (1.5 μm at 1.8 cm/s).

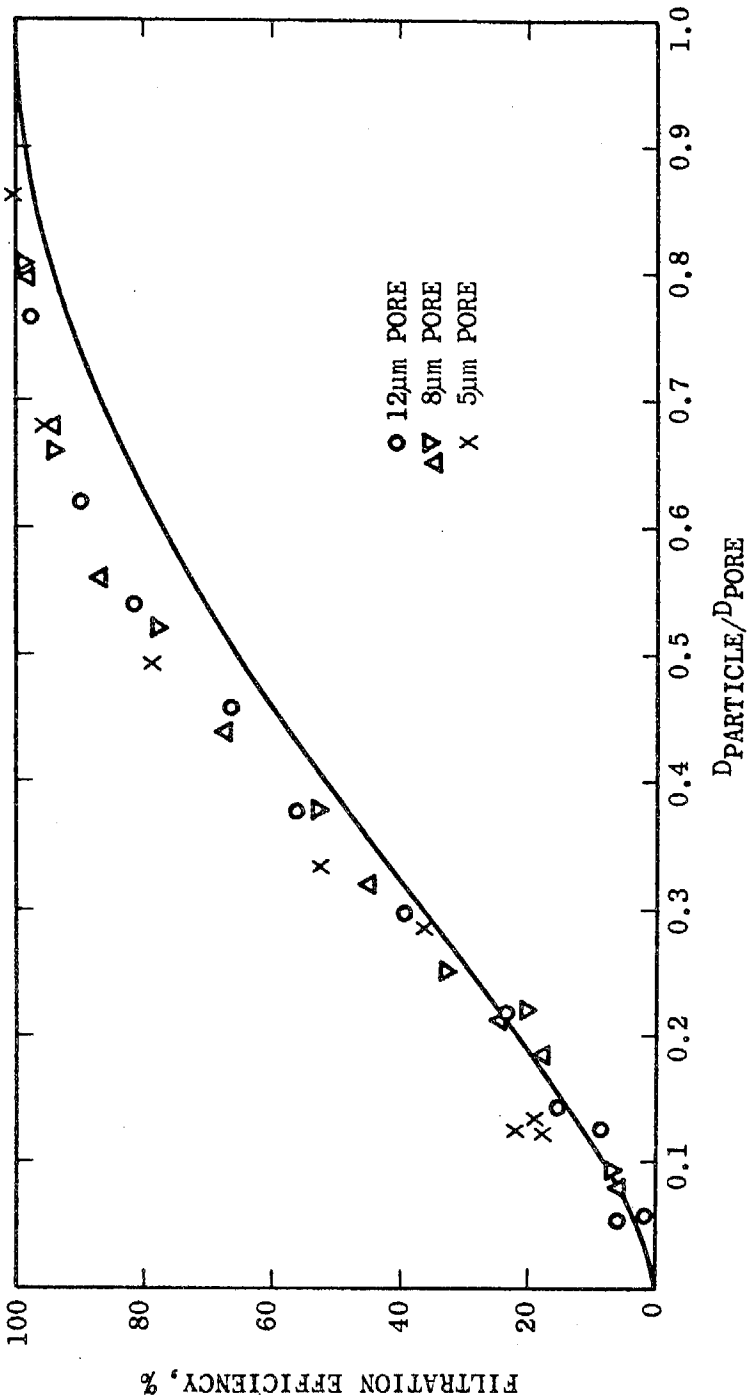

Figure 12. Filtration efficiencies for liquid particles at face velocity of 1.8 cm/s vs. dimensionless particle size. The line is theoretical interception in the creeping flow approximation.

GREASE - COATED FILTERS

Preparation

The particle bounce phenomenon observed in the present work has also been detected in ambient sampling with the SFU. Cahill, et al.,[20] have attempted to reduce the problem by coating the filters with Apiezon vacuum grease. Coated filters, kindly supplied by the U.C. Davis group, have been included in the present laboratory aerosol testing.

The coatings were applied by dipping the filters in a dilute solution of Apiezon L grease in toluene. The grease thickness was determined by weighing and the solution concentration chosen to maximize the thickness without significantly clogging the pores as judged by the pressure drop. Two sets of filters were tested here, lot 51D7B83 with a grease thickness of $(9 \pm 3)\,\mu g/cm^2$, and an average increase of pressure drop (measured during the work reported below) of 14%. The second lot, 51D7B36 had a grease thickness of 17 $\mu g/cm^2$ and an increase in pressure drop of 4.5%.

Filtration Efficiencies of Coated Filters

Filtration efficiencies were measured at 8.4 cm/s on 8 µm filters from lot no. 51D7B36 which were coated with Apiezon grease. As shown in Fig. 13, the liquid particle (glycerol) points agree well with the dashed line representing the corresponding data taken on uncoated 8 µm filters from a similar lot, 51D7B55 (see Fig. 10). The solid particle efficiencies (potassium biphthalate) are much closer to the liquid particle curve than in the uncoated filter case, but are still systematically lower, for example, 27% lower at 3 µm diameter.

Similar results were found for grease-coated 8 µm filters from lot 51D7B83. At 8.4 cm/s the solid particle efficiencies were about 23% less than for liquid particles. At 1.8 cm/s, solid particle efficiencies were about 15% less than for liquid particles. This indicates less bounce at lower face velocity.

The above results show that the grease coating reduces particle bounce by a large factor but not completely. The reason for the remaining excess penetration by solid particles is not known. Perhaps the grease coating does not completely cover the critical surface area near the hole.

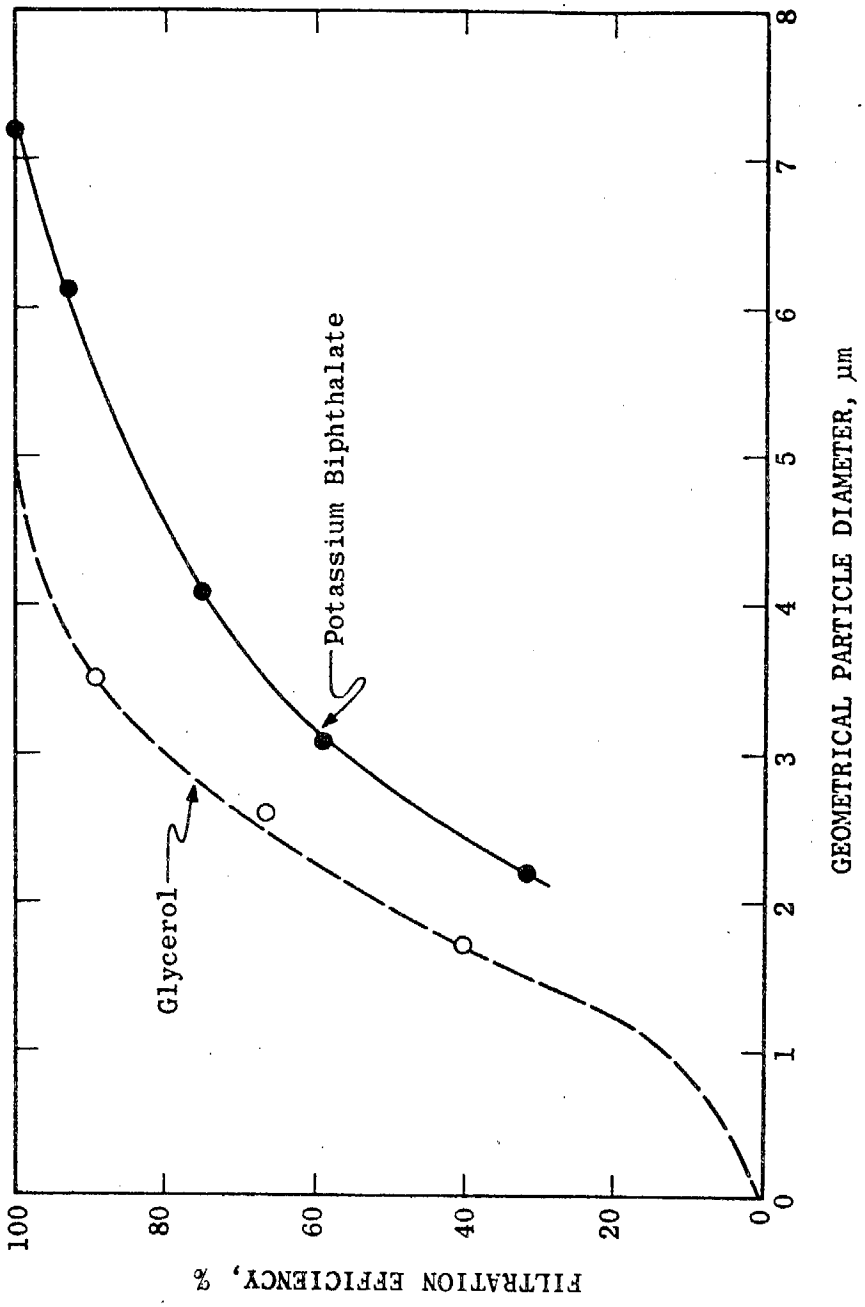

Figure 13. Filtration efficiencies at 8.4 cm/s face velocity for liquid (open circles) and solid particles (solid circles) through 8 µm grease-coated filters from lot 51D7B36. The solid line is an eye-fitted curve; the dashed line is an eye fit to the data on uncoated filters from lot 51D7B55 (Figure 10).

Loading Effects

Since the grease coating eliminates most of the particle bounce, solid particles build up deposits on the filters. Indeed, minute by minute increases in efficiency and pressure drop could be seen under the conditions of the experiment. Data from the optical counters yielded the filtration efficiency at a given time and from the accumulated counts the number of particles deposited on the filter could be determined.

Fig. 14a shows the filtration efficiency vs. number of particles deposited on an 8 μm grease-coated filter for 2, 3 and 7 μm potassium biphthalate particles. The efficiencies for 2 and 3 μm particles show a steep initial rise, then approach a common asymptotic trend. It is remarkable that the effect of only a few particles per pore is significant. The curve for the 7 μm particles is difficult to interpret; the diameter of these particles is near the pore size. Fig. 14b shows the pressure drops recorded during the same runs. The 2 and 3 μm curves have a slight inflection, while the 7 μm particles are very effective in plugging the pores. Again, only a few particles per pore result in significant pressure rise.

Data for simultaneous loading by 2 μm glycerol particles and 2.68 μm latex particles are shown in Fig. 15a and 15b. The filter had a slight loading prior to the run of $0.8 \cdot 10^6$, 4 μm dia. and $2.7 \cdot 10^6$, 3 μm dia. potassium biphthalate particles. Glycerol particles were much more effective in loading greased filters than uncoated filters. The reason was evident under the microscope. Glycerol wets uncoated Nuclepore, the particles spreading out into a low puddle. The glycerol particles do not wet the greased surface, presenting a much higher droplet profile.

Because it is difficult to predict loading effects for ambient air, filters were loaded by operating a sampler near an open window in the Berkeley laboratory. The sampling was interrupted periodically, the filter weighed, and the filtration efficiency determined with laboratory aerosol.

Results for an 8 μm filter are shown in Fig. 16a. The efficiency for liquid particles rises steeply for very light ambient loading. The efficiency for solid particles is initially flat, possibly even dropping slightly. This may be due to the opposing effects of bounce off as the grease is covered with ambient particles and loading by accumulated particles. The pressure drop (Fig. 16b) jumped abruptly beyond 300 μg on the filter.

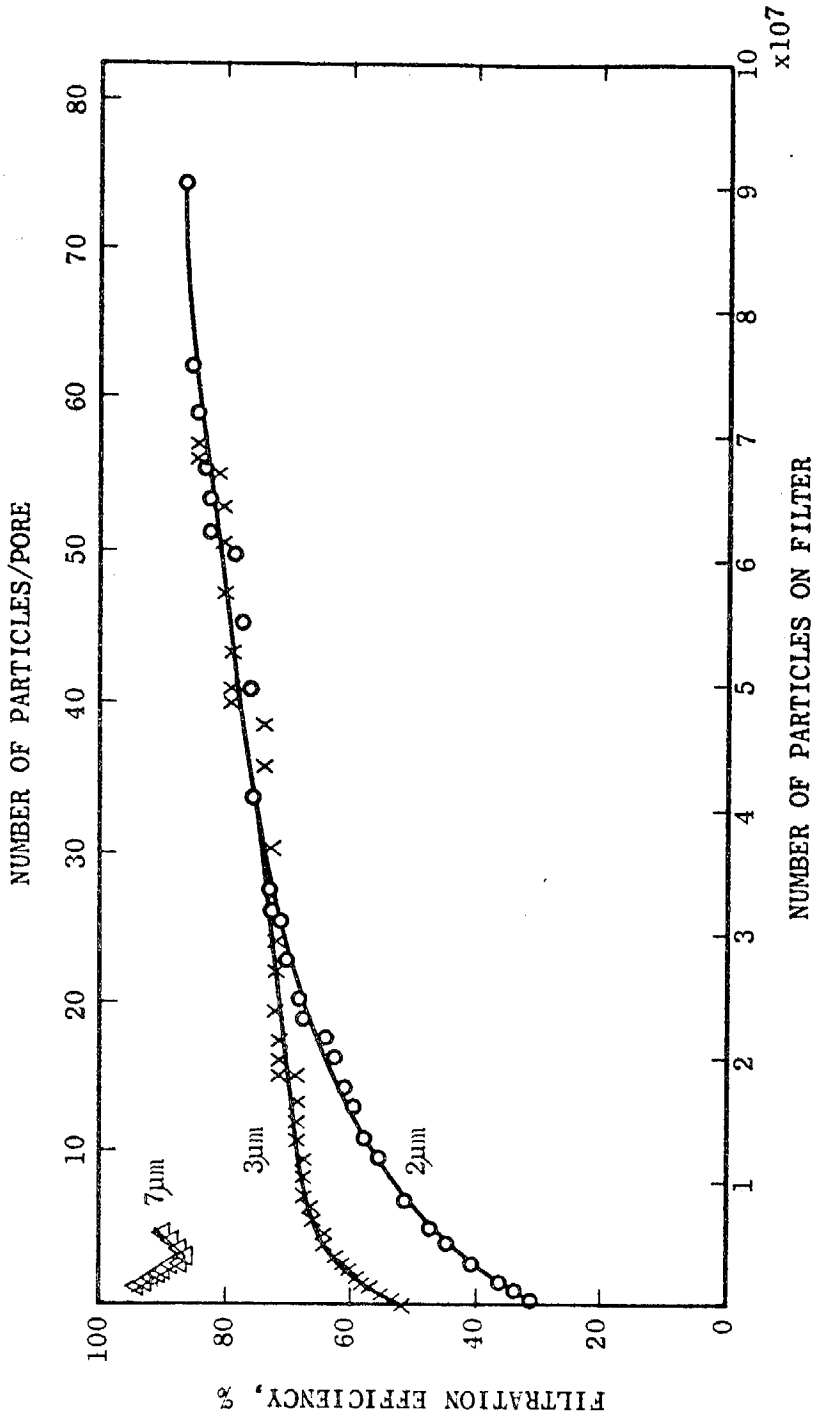

Figure 14a. Filtration efficiency vs. particle loading on an 8 μm grease-coated filter from lot 51D7B36. The eye-fitted curves are labelled with the diameter of the solid, potassium biphthalate particles.

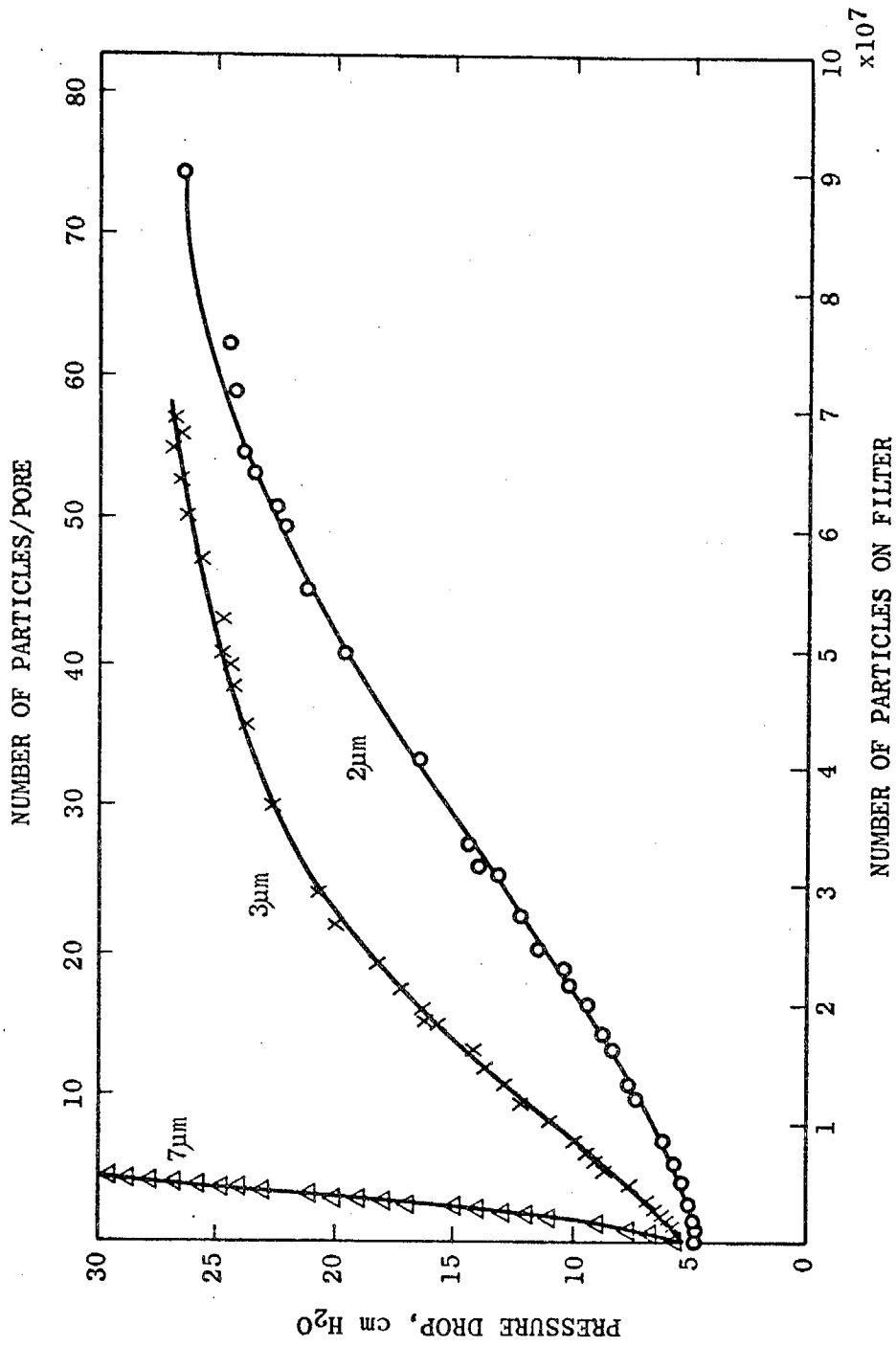

Figure 14b. Pressure drop vs. particle loading for the same runs as in Figure 14a.

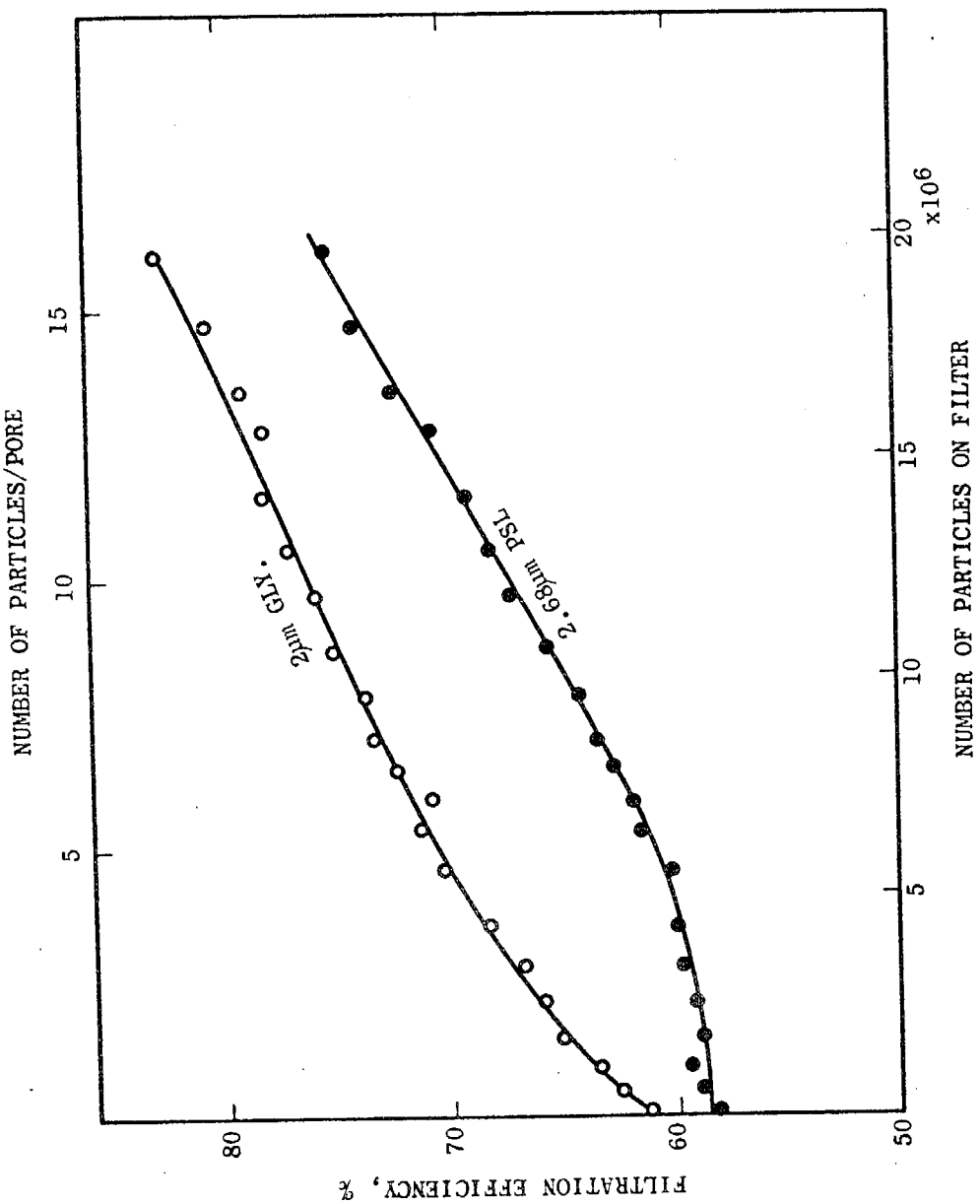

Figure 15a. Filtration efficiency of an 8 μm grease-coated filter from lot 51D7B36 for simultaneous loading by liquid (glycerol) and solid (polystyrene latex) particles. The filter had a light loading before the run as explained in the text.

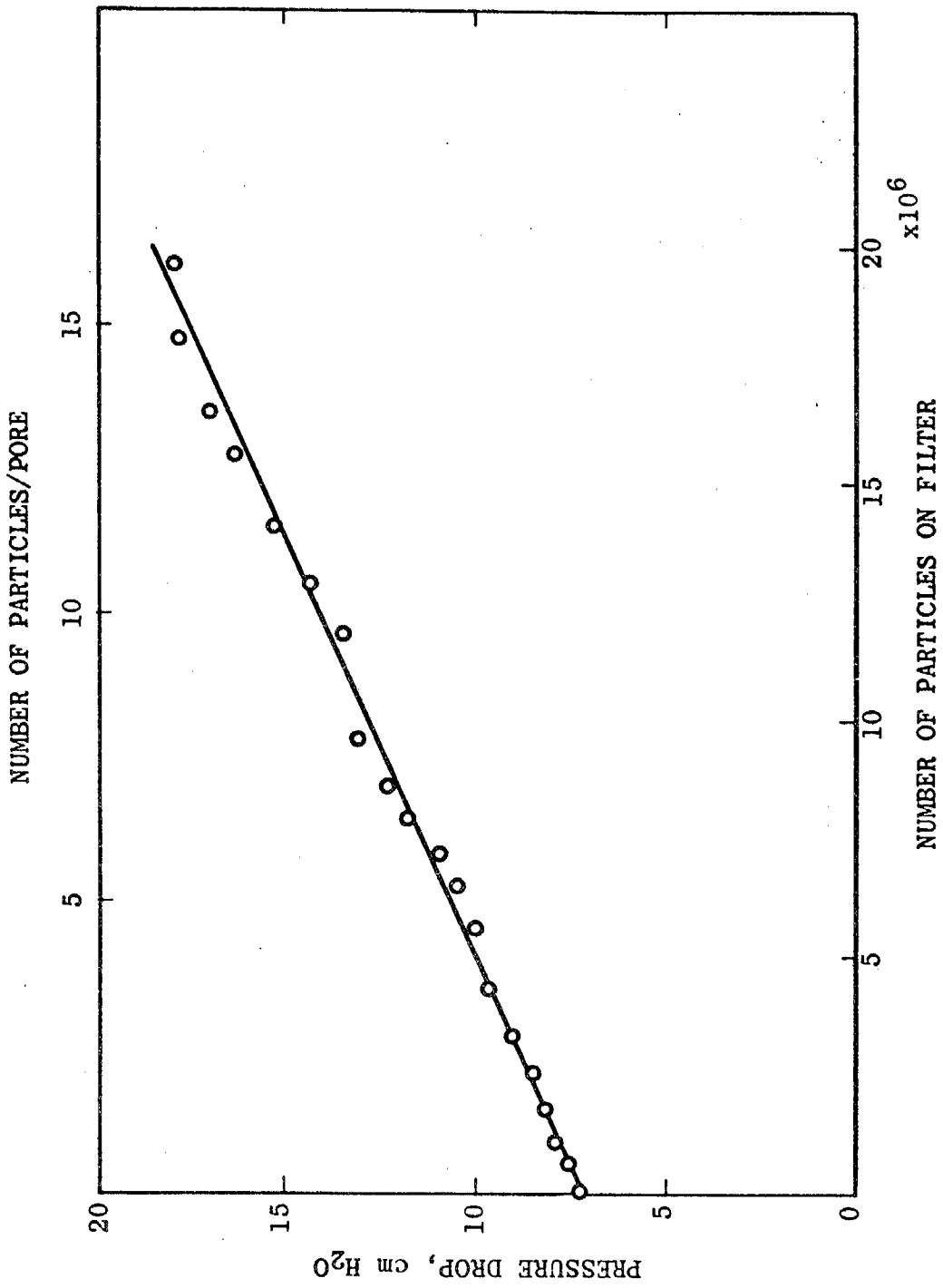

Figure 15b. Pressure drop vs. particle loading for the same runs as in Figure 15a.

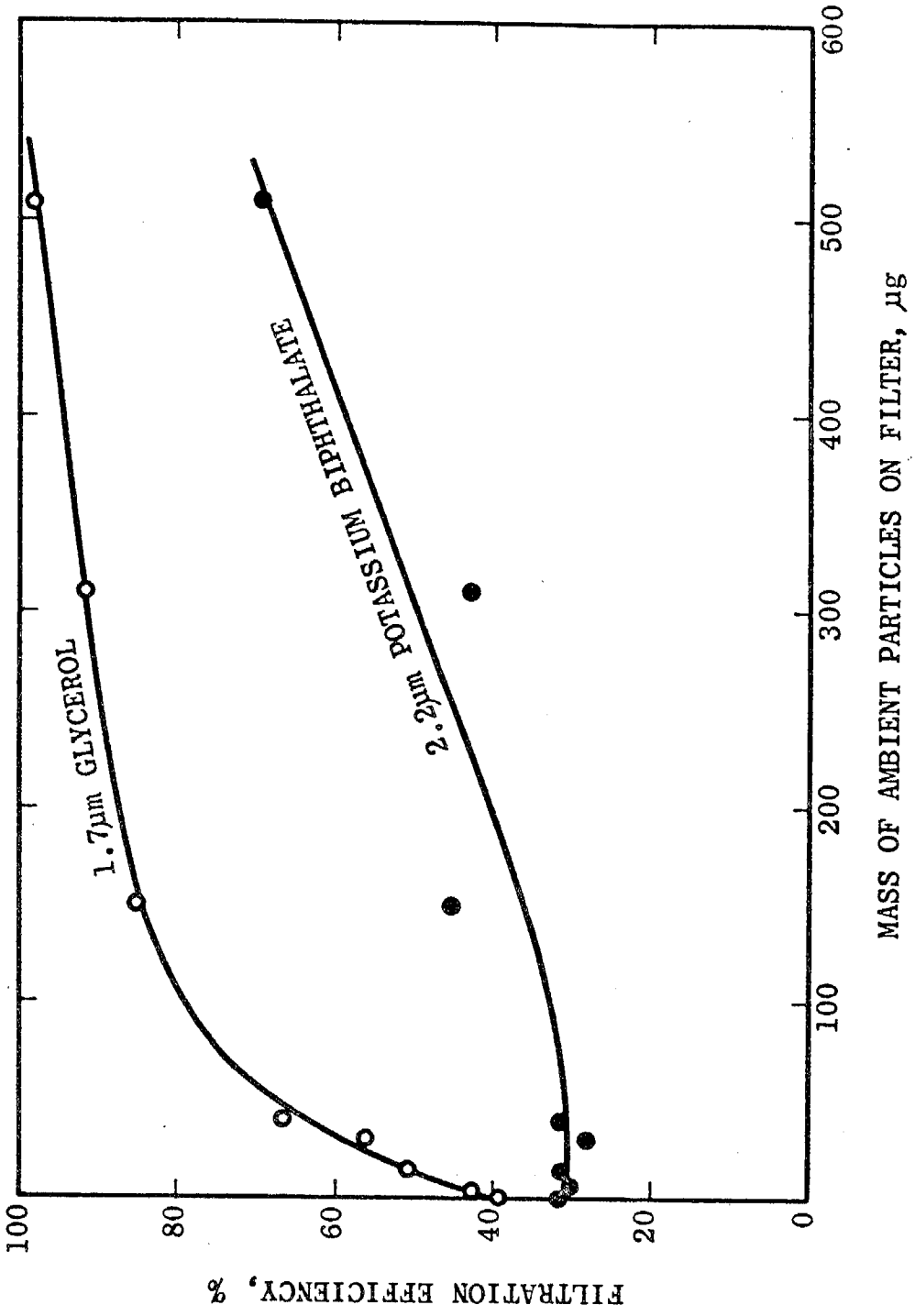

Figure 16a. Filtration efficiencies of an 8 µm grease-coated filter from lot 51D7B36 vs. loading by ambient particulate matter.

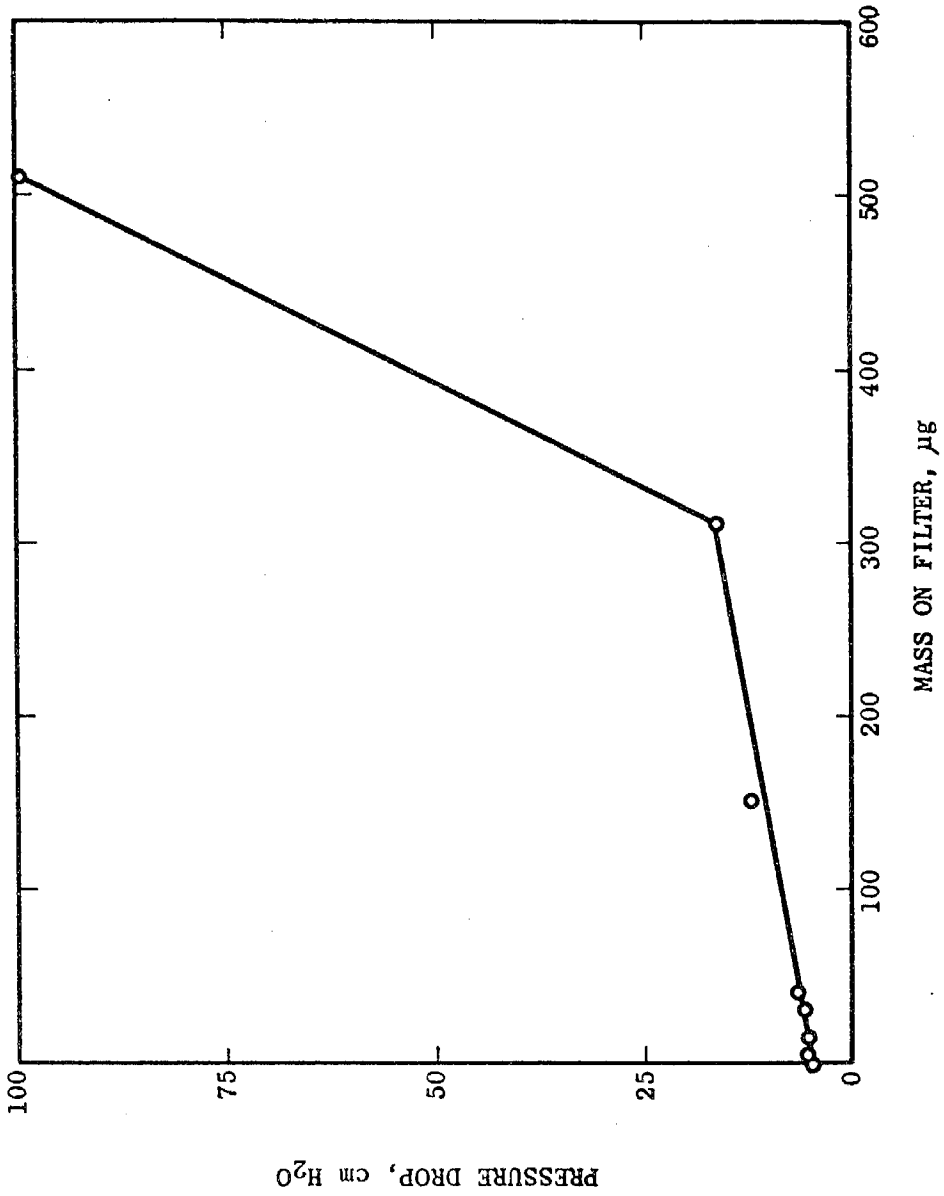

Figure 16b. Pressure drop vs. loading for the same runs as in Figure 16a.

Since bounce off was less important for the 5μm pore size filters, the later were potentially useful even uncoated. Therefore loading data were taken on uncoated 5μm filters (Fig. 17a and 17b). The efficiencies change less rapidly than for glycerol on coated 8μm filters (Fig. 16a) and the solid particle curves parallel that for liquid. The pressure drop again rose more steeply near the end of the run.

OPTIMUM CONDITIONS FOR AMBIENT SAMPLING

Two filters were chosen as the most promising as the large pore size filter to be used in the first stage of the SFU for ambient air sampling. These were the 8μm grease coated filters and the 5μm filters which showed the least bounce off effect of the uncoated filters. The selected filters were tested with laboratory aerosol before and after loading with ambient aerosol at two different flow rates. A target loading of 200-300μg was chosen as sufficient for gravimetric and x-ray measurements.

The results for the 8μm grease coated filter are graphed in Fig. 18. At a face velocity of 8.4 cm/s the loading increased the spread between the efficiencies for liquid and solid particles to more than 2μm (1.8 vs. 4.0μm respectively). At 1.8 cm/s the spread after loading was only 0.7μm. For the 5μm uncoated filter (Fig 19), the 8.4 cm/s face velocity again produced a large bounce off effect. At 1.8 cm/s the solid and liquid curves responded to loading almost equally, both however, shifting more than the corresponding 8μm coated filter curves.

It is evident from the data that a 8.4 cm/s face velocity is too high regardless of the choice of filter. The operating flow rate should be maintained at about 1.8 cm/s or lower. This restricted flow rate implies a typical sampling time of about one week. ($15m^3$) Of the two filter types, the 8μm grease-coated filter gave the least shift with loading. The cutpoint is also closer to the currently favored value of 2.5μm aerodynamic diameter.

TESTS OF THE STACKED FILTER UNIT

Filter Support Screen

The Stacked Filter Unit devised by the U.C. Davis group and sold commercially uses

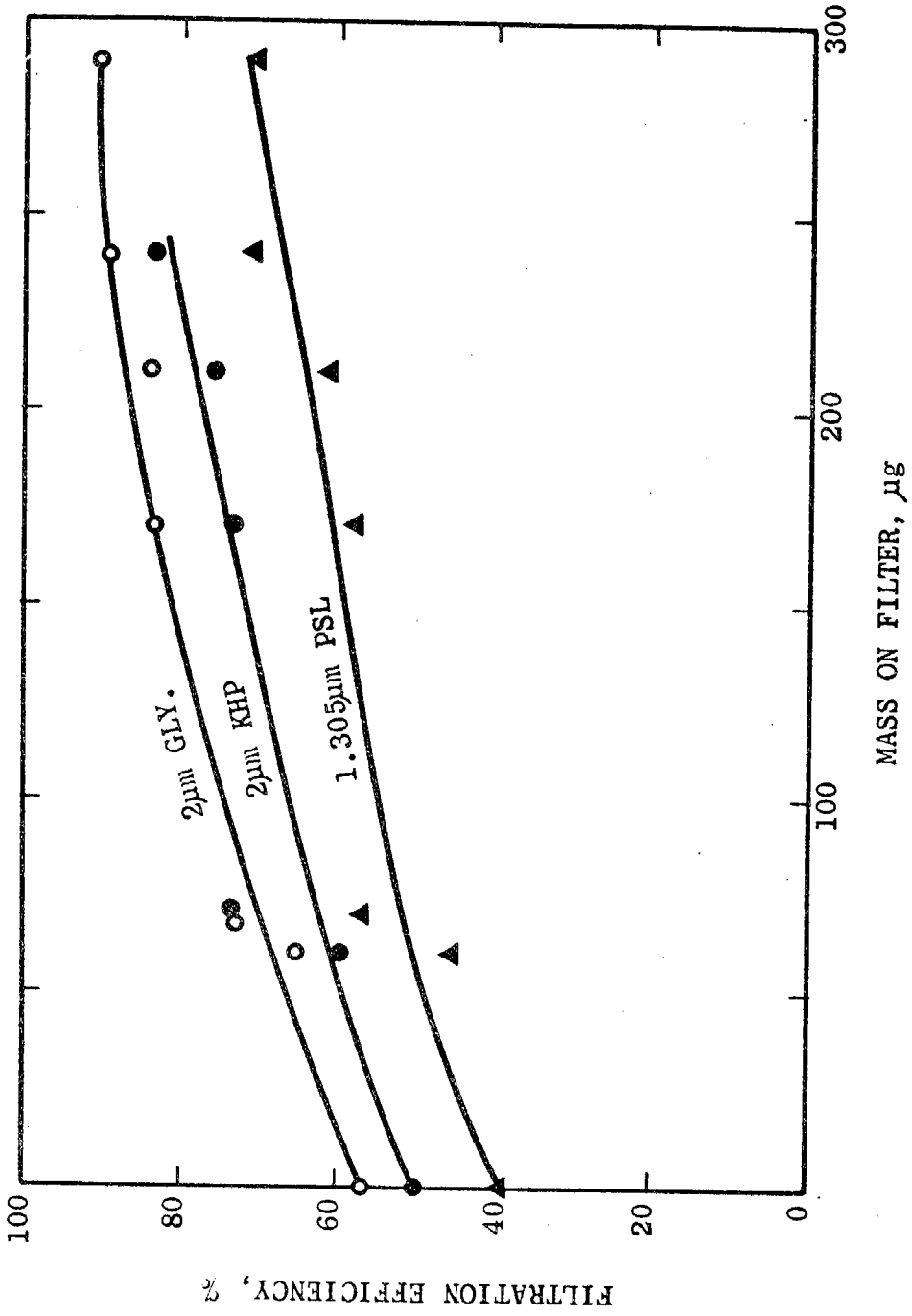

Figure 17a. Filtration efficiencies of a 5 µm uncoated filter from lot 57A8A43 vs. loading by ambient particulate matter.

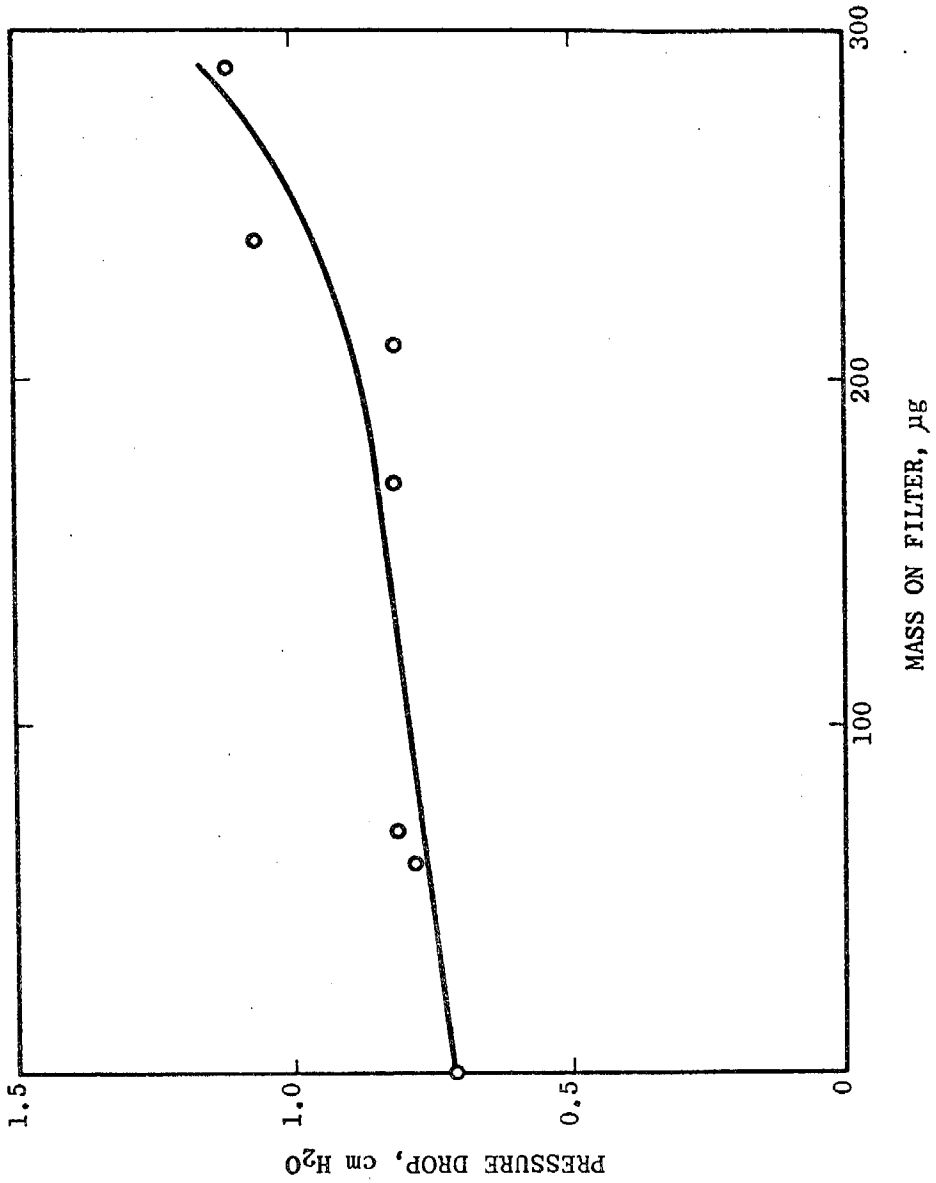

Figure 17b. Pressure drop vs. loading for the same runs as in Figure 17a.

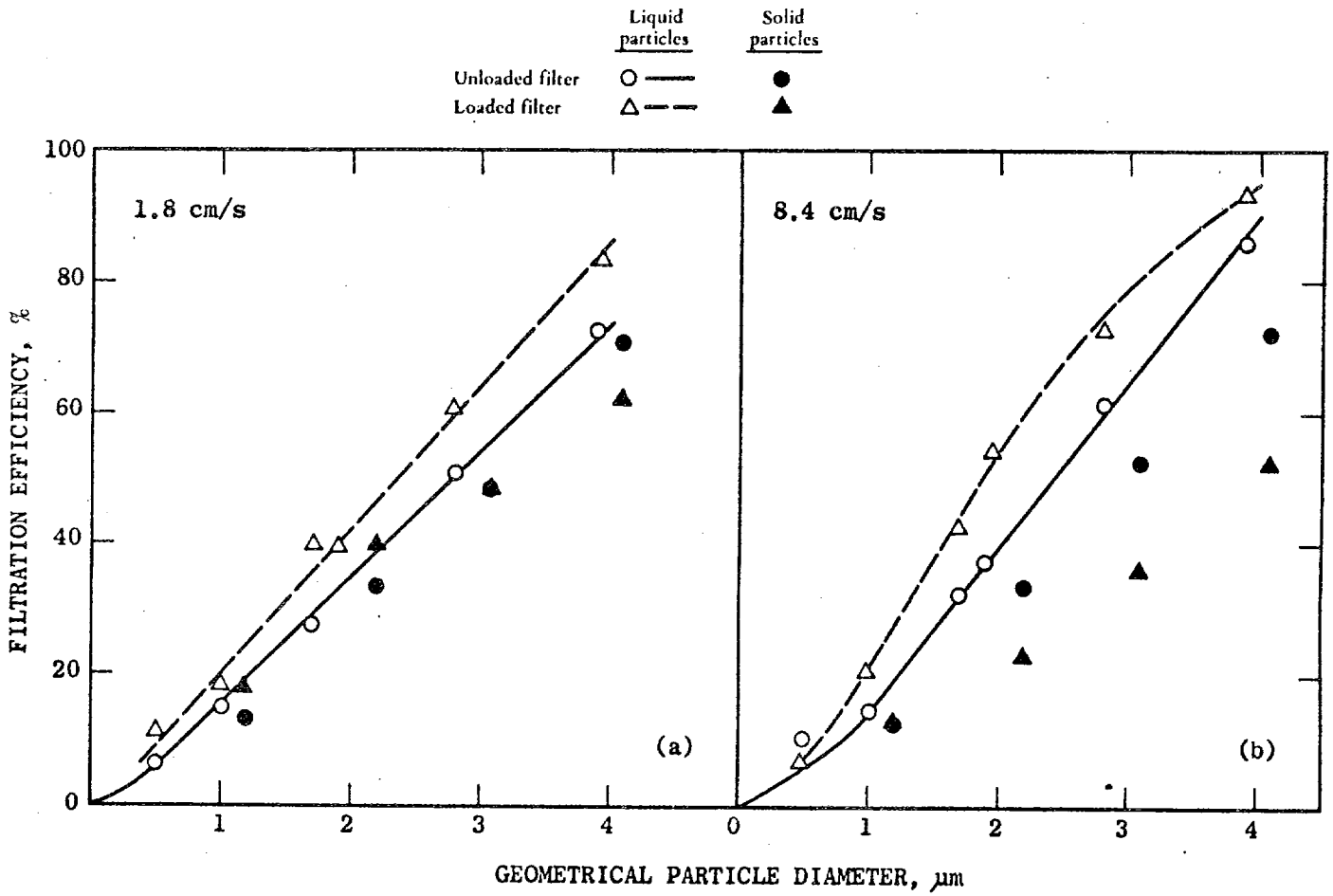

Figure 18a,b. Filtration efficiencies of 8 μm grease-coated filters from lot 51D7B83 before and after loading with 17 $\mu g/cm^2$ of ambient particulate matter. The face velocities were (a) 1.8 cm/s and (b) 8.4 cm/s.

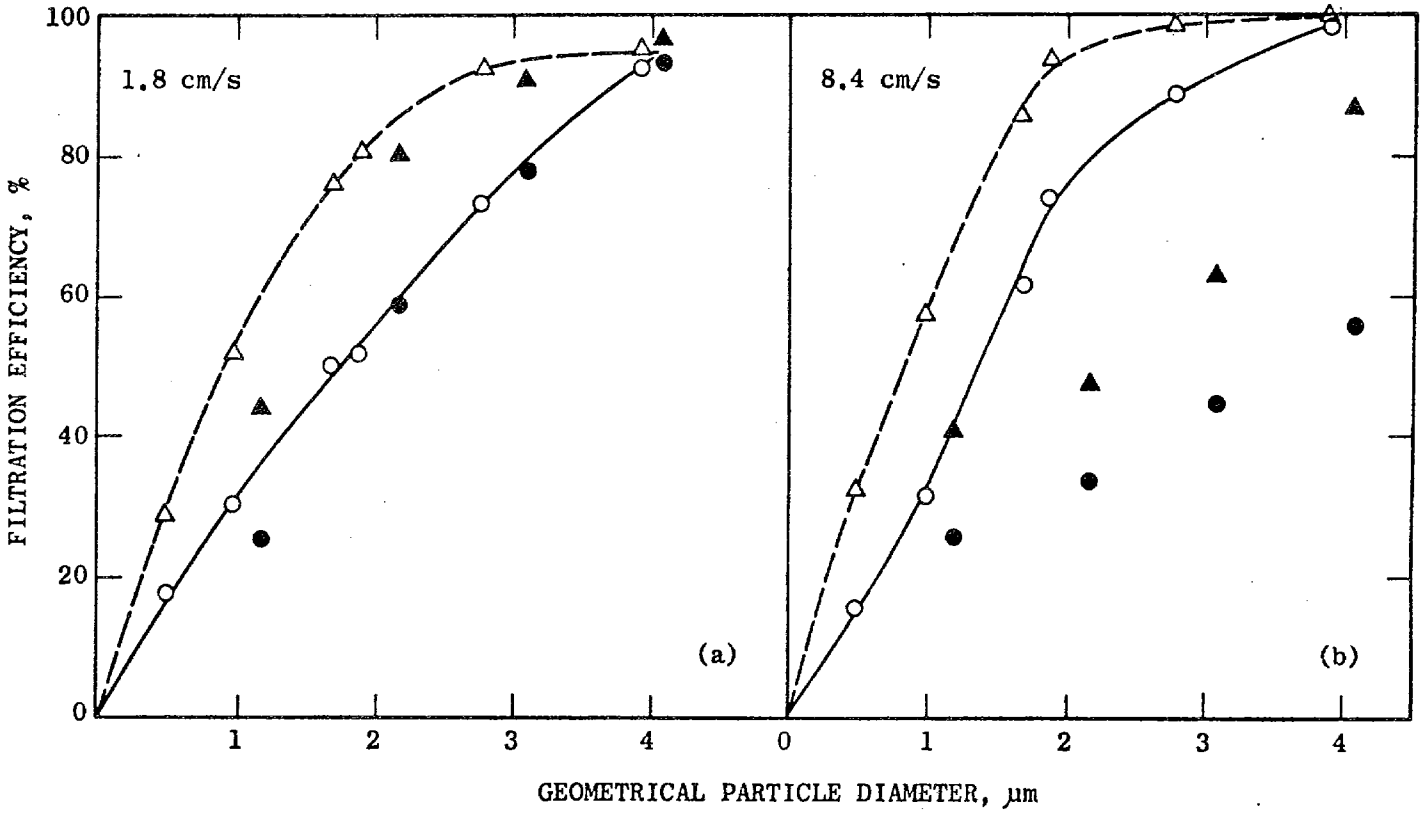

Figure 19a,b. Filtration efficiencies of 5 μm uncoated filters from lot 57A8A43 before and after loading with 21 $\mu g/cm^2$ of ambient particulate matter. Symbols and lines are explained under Figure 18.

a standard Nuclepore filter holder assembly whereby the first, large-pore filter is supported on a plastic grid. Since the particles penetrating the coarse filter must traverse the support grid, possible losses on the grid are of concern. The grid consists of two sets of ribs at right angles. The crossings cause abrupt changes in the air flow which could cause impaction.

Losses on the grid were measured by sampling monodisperse glycerol particles containing a uranine tracer. The 8 μm coarse filter, 0.4 μm fine filter and the grid were washed in solvent and the uranine quantitated on a fluorometer. At a face velocity of 5.8 cm/s, the grid deposit ranged from 13% for 0.8 μm particles down to 2.2% for 7.3 μm particles. (The latter is 50% of the particles penetrating the coarse filter). The support grid was replaced by a 16 mesh stainless steel screen. Screen deposits were then found to be 1.2% at 8.4 cm/s and 1.5% at 1.2 cm/s for 2.5 μm glycerol particles.

An alternative at the low flow rates used here is simply to eliminate the support screen. The polycarbonate plastic can easily support the pressure. The edges should be clamped securely against an O-ring.

Flow Controller

Four air samplers designed for the SFU, Sierra Model 202-2F,* were tested. Each unit was first subjected to an overall check for leaks by placing rotameters at the intake and exhaust to see if the flows are equal. Typically, they are not, the cause being loose connections. The panel flow meter (a rotameter) was calibrated against a wet test meter and found to be linear with an rms accurracy of 15% at 2 L/min and 4% at 10 L/min.

The flow controller was tested by placing a needle valve at the intake to produce a variable pressure drop. The flow rate is plotted against the pressure drop in Fig. 20. The drop off above 14 to 15 in. Hg is typical. At lower flow rates the deviation from the set flow varies with the unit, but is within 5 to 10%. The flow controller performance is therefore satisfactory for the SFU.

---

* Sierra Instruments, Inc., Carmel Valley, CA.

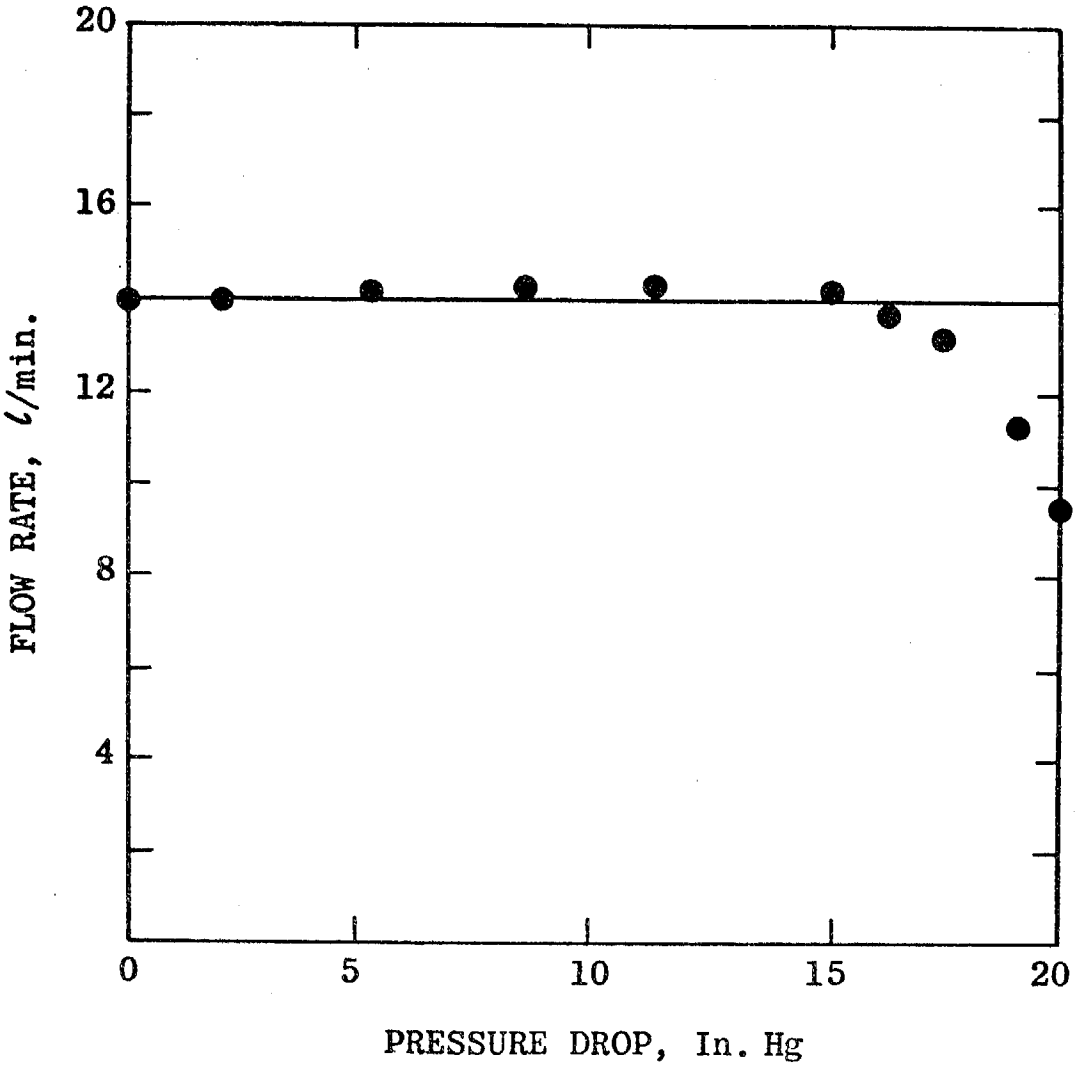

Figure 20. Performance of the Sierra mechanical flow controller for the SFU.

CONCLUSIONS

The physical parameters of the large pore size Nuclepore filters to be used as the first, coarse filter in the SFU are uniform within a given filter lot; however, variation between lots necessitates knowledge of the pore size and pore density for accurate work. The pressure drop is a useful empirical indicator of the filter parameters. A formula has been developed for the calculation of the pressure drop from the parameters and the flow rate.

For liquid particles the filtration efficiency increases weakly with face velocity. Most of the particle deposition is attributed to interception. A theoretical calculation of interception in the creeping flow approximation compares well to the data. Therefore the particles are essentially sized geometrically rather than aerodynamically.

Efficiencies for solid particles are much lower than for liquid particles. Moreover, the efficiency for solid particles decreases with increasing face velocity, indicating that the particles bounce from the filter surface and penetrate the pores. Coating the filters with grease greatly reduces but does not completely eliminate particle bounce.

Loading of the filters with laboratory-generated particles and by particles from ambient air shows that the efficiency and pressure drop change significantly for deposits of only a few particles per pore. The optimum sampling conditions were found to be at 1.8 cm/s face velocity with an 8 μm grease coated filter. This implies a minimum sampling period of about one week.

The present work shows that the Stacked Filter Unit should not be regarded as a routine monitoring tool. Particles are sized geometrically rather than aerodynamically and the cutoff is not sharp. Filters must be grease-coated to eliminate particle bounce. A low flow rate is necessary, requiring a sampling period of a week. Within these limitations, the SFU is an inexpensive size-selective sampler which could be useful for special projects.

ACKNOWLEDGEMENTS

We thank Professor Simon Goren for his continuing interest in this work and for participation in the theoretical work. David Plotkin assisted with the early phases of the experimental work. We thank the Nuclepore Corp. for friendly cooperation and discussions. Dr. Tom Cahill kindly supplied an SFU and greased filters.

REFERENCES

1. The Current Status of Particulate Matter Monitoring, W. John, Third Interagency Symposium on Air Monitoring Quality Assurance, Berkeley, CA, May 18-19, 1977.

2. Deposition and Retention Models for Internal Dosimetry of the Human Respiratory Tract, Task Group on Lung Dynamics, Health Physics 12, 173-207 (1966).

3. Atmospheric Visibility Related to Aerosol Mass Concentration: A Review. R.J. Charlson, Envir. Sci. Technol. 3, 913-918 (1969)

4. Characterization of Aerosols in California (ACHEX), G.M. Hidy, et al. Final Report, ARB Contract No. 358, Vol. I, Summary, Sept. 30, 1974, revised April, 1975.

5. Application of the Dichotomous Sampler to the Characterization of Ambient Aerosols, T.G. Dzubay, R.K. Stevens and C.M. Peterson, in X-Ray Fluorescence Analysis of Environmental Samples, T.G. Dzubay, ed., Ann Arbor Science, Ann Arbor, MI, 1977, pp 95-105.

6. Size-Selective Monitoring Techniques for Particulate Matter in California Air, W. John, G. Reischl and J.J. Wesolowski. Final Report, Interagency Agreement ARB A5-00487, February, 1978.

7. A High-Volume Sampler for the Determination of Particle Size Distributions in Ambient Air, D.M. Bernstein, M.T. Kleinman, T.I. Kneip, T.L. Chan and M. Lippmann, J. Air Poll. Control Assoc. 26, 1069-1072 (1976).

8. Analysis of Respirable Fractions in Atmospheric Particulates via Sequential Filtration, T.A. Cahill, L.L. Ashbaugh, J.B. Barone, R.A. Eldred, P.J. Feeney, R.G. Flocchini, C. Goodart, D.J. Shadoan and G.W. Wolfe, J. Air Poll. Control Assoc. 27, 675-679 (1977).

9. A Two Stage Respirable Aerosol Sampler Using Nuclepore Filters in Series, R.D. Parker, G.H. Buzzard, T.G. Dzubay and J.P. Bell, Atmos. Envir. 11, 617-621 (1977).

10. Anomalous Filtration of Solid Particles by Nuclepore Filters, W. John, G. Reischl, S. Goren and D. Plotkin, Atmos. Environ. 12, 1555-1557 (1978).

11. Aerosol Filtration by Means of Nuclepore Filters: Structural and Filtration Properties, K.R. Spurny, J.P. Lodge, Jr., E.R. Frank and D.C. Sheesley, Envir. Sci. Technol. 3, 453-464 (1969a).

12. Aerosol Filtration by Means of Nuclepore Filters: Aerosol Sampling and Measurement, K.R. Spurny, J.P. Lodge, Jr., E.R. Frank and D.C. Sheesley, Envir. Sci. Technol. 3, 464-468 (1969b).

13. Aerosol-Size Spectra by Means of Membrane Filters, O.T. Melo and C.R. Phillips, Envir. Sci. Technol. 8, 67-71 (1974).

14. Guide for Respirable Mass Sampling, Aerosol Technology Committee, American Industrial Hygiene Association. Amer. Indust. Hyg. Assoc. J. 31, 133-137 (1970).

15. Elemental Analysis of Environmental Samples, T.A. Cahill in New Uses of Ion Accelerators, J. Ziegler, ed., Plenum Press (1975).

16. Low Reynolds Number Hydrodynamics, J. Happel and H. Brenner, 2nd revised Edn., Noordhoff International, Leyden, The Netherlands, (1973), pp. 150-153.

17. Ibid, p. 34

18. Generation of Monodisperse Aerosol Standards, R.N. Berglund and B.Y.H. Liu, Envir. Sci. Technol. 7, 147-153 (1973).

19. Size Considerations for Establishing a Standard for Inhalable Particles, F.J. Miller, D.E. Gardner, J.A. Graham, R.E. Lee, Jr., W.E. Wilson and J.D. Bachmann, J. Air Poll. Contr. Assoc. 29, 610-615 (1979).

20. T. Cahill, private communication.